IMPORTANT NOTICE

BAROCLINIC INSTABILITY AS AN INITIAL VALUE PROBLEM

A thesis presented

by

Brian Francis Farrell

to

The Division of Applied Sciences

in partial fulfillment of the requirements

for the degree of

Doctor of Philosophy

in the subject of

Applied Mathematics

Harvard University

Cambridge, Massachusetts

July, 1981

Preface

Baroclinic instability is recognized as the major causal factor in what is generally regarded as "weather" in midlatitudes: the synoptic scale cyclonic disturbances. Equally as important is the role the waves resulting from this instability play in the maintenance of the general circulation of the atmosphere. As a result this mechanism has been extensively studied since its discovery in the pioneering work of Charney (1947) and Eady (1949). This work explores the behavior of waves resulting from an initial disturbance to a baroclinic fluid in two limits: that of long time and of short time. In the limit of long time, the asymptotics of a localized perturbation to the canonical model of Charney is developed and related to the observed spacial scales and growth of cyclones. The short time limit is examined to gain an understanding of the manner in which the asymptotic wave is set up from an initial disturbance.

My interest in this problem was stimulated by work done on various aspects of baroclinic instability under the guidance of my advisor Professor Richard Lindzen who suggested the study of meteorology and for whose aid and encouragement through the years of my apprenticeship I am deeply grateful.

I would also like to express appreciation for a summer fellowship from the National Center of Atmospheric Research to attend the 1978 Advanced Study Program colloquium at NCAR, where some of these ideas were first developed. I thank Dr. Arthur Rosenthal for kindly checking approximations related to his work and for lending his computer graphics

expertise and Dr. R. Pierrehumbert for allowing me to attend his stimulating lectures at Massachusetts Institute of Technology. The work was supported by NSG GrantATM-78-23330 and by NASA Grant NGL-22-007-228 at Harvard University.

TABLE OF CONTENTS

LIST OF FIGURES

PART I

PART II

SYNOPSIS

This study examines the initial value problem in baroclinic instability from two perspectives, the limit of long time and the interval in time of the early growth. Part I contains the solution of the long time asymptotic behavior of localized perturbations in various model flows. Part II concentrates on the set up of the normal mode from a perturbation.

PART I: PULSE ASYMPTOTICS OF THE CHARNEY BAROCLINIC INSTABILITY PROBLEM

CHAPTER I INTRODUCTION

Since its discovery in the work of Charney (1947) and Eady (1949), baroclinic instability has been accepted as a major source of synoptic scale disturbances in midlatitudes. The normal mode method of analysis used in these early works and in most subsequent investigations makes the assumption of a solution infinitely periodic in the horizontal direction and determines the space independent growth rate as an eigenvalue of the resulting system of equations. The wavelength of the disturbance most rapidly growing in time is then compared with observed synoptic cyclone scales. The agreement found encourages the identification of these features with baroclinic instability. However, this identification requires that the response of the baroclinically unstable fluid to an initial perturbation, which is most likely localized in space, will evolve into normal mode form. Whether this happens can be decided within the restrictions of linear theory by solving the appropriate initial value problem. In the case investigated here it is found that as a function of distance from the initial perturbation, widely different space scales dominate the solution, calling into question the identification of maximally time growing normal mode wavenumber with the scale of synoptic features.

As it is usually formulated, the IVP requires finally the double inversion of a Fourier transform in space and a Laplace transform in time, in general, a formidable task even for the simplest of models. Progress has been made in the asymptotic evaluation of these integrals for large time, in work done in connection with plasma instabilities (Briggs, 1964). It is found that this limit is determined by the linear dispersion relation generalized to complex frequency and wavenumber. An important conceptual

distinction is pointed out by the analysis -- that between the so-called absolute and convective instabilities. In the former the response continues to grow in time at every point which has been reached by the travelling pulse; in particular, it continues to grow at the point of excitation. In the latter the instability is carried along with the flow so that despite its constantly increasing ampliutde, at any fixed point the disturbance eventually decreases; in particular, at the point of the excitation the effects of perturbation are eliminated after finite time.

Absolute instability has been found for sufficiently small shear in the two-layer model on an f-plane and on the β-plane (Merkine, 1980). The Eady problem was examined by Simmons and Hoskins (1979) and found to have no absolute instability. These model flows have the virtue of possessing dispersion relations expressible in simple analytic form, but are limited in that the structure of these dispersion relations, which is of less consequence in picking out most rapidly growing in time normal modes, is crucial to the asymptotics of pulses. In the hierarchy of baroclinic models the Charney problem is the simplest one to possess at least in modified form most of the features of realistic dispersions from global models (Simmons and Hoskins, 1976; Geisler and Garcia, 1977). Unfortunately, the solution of the Charney model is in terms of hypergeometric functions and yields no exact closed form dispersion relation. In what follows, a highly accurate approximate is used to extend pulse asymptotic results to this case.

It should be borne in mind that these linear asymptotics are valid only after an unspecified long time has elapsed since the original perturbation; it is possible that for some initial conditions the

entire development to nonlinear equilibration of the system which is being modelled may take place before these results obtain validity.

CHAPTER 2 PULSE ASYMPOTOTIC ANALYSIS

2.1 Method of Analysis

The initial value solution is an integral over the normal mode solutions consisting of the exponentially growing modes and their complex conjugate decaying modes plus another integral over a continuous spectrum. The decaying exponentials make no contributions to the long time behavior and the continuous spectrum contributes at most 0(t) (Burger, 1966), so the asymptotic solution takes the form of an integral over the exponentially growing modes:

$$\psi(x,z,t) = \int_{-\infty}^{\infty} dk\ a(k)\ \psi_k(z) e^{i[k\frac{x}{t} - \omega(k)]t} \tag{1}$$

where a(k) = projection of initial condition on the normal mode at k and $\psi_k(z)$ = vertical structure of mode at k. Let

$$\Omega(k) = -\ [k\frac{x}{t} - \omega(k)]\ .$$

Evaluation of (1) is carried out for a frame of reference moving at speed U=x/t by deforming the path of integration in the k plane in the direction of diminishing Ω_i until one of two conditions is met:

1. There is reached a contour for which $\Omega_i \leq 0$ for all k without having encountered a point k_s where $\left.\frac{\partial\Omega}{\partial k}\right|_{k_s} = 0$ and $\Omega_i > 0$ in which case the system is stable as viewed from the translating frame.

2. In performing the deformation of the k contour a saddle point k_s is encountered where:

$$\left.\frac{\partial\Omega}{\partial k}\right|_{k_s} = 0$$

$$\Omega_i(k_s) > 0\ . \tag{2}$$

This is the condition of the so-called pinch singularity. The solution is seen by the observer to be unstable having asymptotic form:

$$\psi(x,z,t) = b(k_s)\psi_{k_s}(z)t^{-1/2}e^{-i\Omega(k_s)t}$$

$$= b(k_s)\psi_{k_s}(z)t^{-1/2}e^{i(k_s x-\omega(k_s)t)} \qquad (3)$$

In particular, if such a saddle point is found for U=x/t=0 with associated $\Omega_i(k_s)>0$ then the system is absolutely unstable with the perturbation envelope at the point of excitation growing as $\Omega_i(k_s)t$. In general, the local maximum envelope growth for any x/t is

$$\nu_i = \omega_i(k_s) - \mathrm{Im}(k_s)\frac{x}{t} \quad . \qquad (4)$$

Examination of the dispersion relation $\Delta(k,\omega)=0$ reveals that, in general, deformation of the k contour results in the associated ω moving in the complex plane. Because of this, the above procedure is visualized best by examining contour plots of complex ω in the complex k plane. Absolute instability, for instance, would exist if for x/t=0 there is a saddle in ω between the real k axis and the $\omega_i=0$ contour.

The pulse shape is found by plotting ν_i against x/t. ν_i is proportional to the log of the envelope magnitude and x/t to the horizontal extent, with proportionality factor t_o, the time at which the snapshot is taken.

The idea of the pinch singularity method is to extend the stationary phase technique for stable wave packets to the complex plane. For absolute instability one would naively expect that the region in k space near where the real group velocity vanishes $\frac{\partial\omega_r}{\partial k_r} = 0$ would make the greatest contribution,

but this expectation must be modified by taking into account the imaginary parts of ω and k as (2) is the complete condition. We will find that for the Charney problem the real group velocity zero points closely approximate the absolute instability real wavenumber. The basic reason for this is that the growth rates are not so large or rapidly varying with wavenumber as to swamp the real dispersive contribution to the stationary phase asymptotics and insofar as these growths are typical we can expect this to be true for other realistic models.

Model flows examined in the past have often been characterized by dispersion relations of the form:

$$\omega = kU + ig(k) \tag{5}$$

with U and g real and U constant, which in fact have $\frac{\partial \omega_r}{\partial k_r} = U$ for all unstable k. The wavenumber selection is in terms of the imaginary variation and the k of largest ω_i, k_m will dominate. Models of this type include the two-level on an f-plane and the Eacy. Insight can be gained by expanding the leading order terms in (5) about $\delta = \frac{x}{t} - U$ to obtain an approximate asymptotic pules (Benjamin, 1961):

$$\psi \simeq \exp\left\{ i\left(\frac{x}{t} - U\right)k_m t + \left[g(k_m) - \frac{\left(\frac{x}{t} - U\right)^2}{2|g''|_{k_m}} \right] t \right\}. \tag{6}$$

Absolute instability is predicted in this approximation when the Gaussian wave packet spreads more rapidly than it advects. The limits of the packet are at:

$$\frac{x}{t} = U \pm \sqrt{2g(k_m)|g''|_{k_m}} \quad . \tag{7}$$

In these cases the group velocity is constant and the spreading of the packet is determined by the magnitude of the maximum growth rate $g(k_m)$ and the packet width, proportional to $|g''|_{k_m}$. The point of maximum growth,

which is the peak of the wave packet, moves at velocity U and has the wavenumber of the most unstable normal mode. Note that the phase speed is also U so that the high or low located at the peak of the packet remains there as the packet propagates. This would not be true for dispersive waves where individual highs and lows move through the packet maximum. Returning to (7), if $x/t<0$, then absolute instability is predicted by this approximation and the saddle point asymptotics will, in general, confirm this.

The Eady problem has a dispersion relation of the form (5). For infinite meridional scale it is:

$$\omega = \frac{k}{2} \pm i\left[k \coth k - \frac{k^2}{4} - 1\right]^{1/2} .$$

Evaluation of (7) suggests that this problem just fails to be absolutely unstable (see Appendix A). The asymptotic pulse is shown in Fig. 1a. Real wavenumber k_r, imaginary wavenumber k_i, and rest frame frequency, ω_r across the pulse are shown in Fig. 1b. Analytic results for the immediate neighborhood of $x/t=0, 1$ confirm that $\lim_{x/t \to 0,1} \nu_i = 0$ and that $\lim_{x/t \to 0,1} k_r = \infty$ (Simmons and Hoskins, 1979). If the meridional scale is not infinite ($\ell \neq 0$) this problem fails to be even marginally absolutely unstable.

In the two-layer model with $\beta \neq 0$, the dispersion relation can be written (Merkine, 1980):

$$\omega = k - \frac{\beta}{k}\frac{k^2+1}{k^2+2} \pm \frac{\left[\varepsilon^2 k^4 (k^4-4) + 4\beta^2\right]^{1/2}}{2k^2(k^2+2)}$$

where ε, the shear parameter, is such that the upper layer flow is $U_1 = 1+\varepsilon/2$, while the lower layer flow is $U_2 = 1-\varepsilon/2$.

The dispersion for real k is shown along with the group speed in Figs. 2a, b for a choice of parameters $\varepsilon=2.0$, $\beta=1.0$, which result in absolute instability. The growth rate ν_i from (4) is plotted in Fig. 2c and the

local wavenumber across the pulse in Fig. 2d. Note that even though $c_g = \frac{\partial w_r}{\partial k_r} > 0$ for all unstable k, the absolute instability is made up of wavenumbers with lower values of c_g.

Qualitatively speaking, the growth rate is small enough that the effect contained in (6) is dominated near the absolute instability by the tendency of zero, or, as in this case, the smallest available, group velocity waves to make up the stationary part of the instability. This effect is even more striking in the examples that follow, where group velocity zero is associated with appreciable growth rate. Note that these pulses have finite upstream velocity so that the addition of a sufficiently large uniform zonal velocity to the basic flow would make the absolute instability convective and the same pulse would then be interpreted as a spatially amplifying packet.

2.2 The Charney Problem

The Charney problem describes quasi-geostrophic perturbations of a zonal flow with velocity a function of height only, U(z). The scale height H and Brunt-Vaisala frequency N are constant. The effects of sphericity are confined to the β-plane approximation. In what follows, the notation of Lindzen, et al. (1980) will be used.

Conservation of pseudo-potential vorticity requires for the stream function Ψ:

$$\psi_{zz} + \{\frac{q(y)}{U-c} - \frac{\alpha^2}{\varepsilon} - \frac{1}{4H^2}\}\psi = 0 \qquad (8)$$

where

$\Psi = \psi(z)\ e^{z/2H} e^{ik(x-ct)}$

$\alpha^2 = k^2+\ell^2$, the sum of square zonal and meridional wavenumbers

$q(y) = \frac{\beta}{\varepsilon} + \frac{U_z}{H} - U_{zz}$

$H = \frac{RT_o}{g}$, the scale height

$\varepsilon = \frac{f^2}{N^2}$

f = Coriolis parameter

$\beta = \frac{\partial f}{\partial y}$

x = eastward direction

y = northward direction

z = height

The boundary condition requires that the vertical velocity vanish at the ground

$$\psi_z + \frac{\psi}{2H} - \frac{U_z}{U-c}\psi = 0, \quad z = 0 \qquad (9a)$$

and that ψ approach zero at infinity

$$\lim_{z \to \infty} \psi(z) = 0 . \tag{9b}$$

We assume a linear shear $U(z)=mz$, and make the following nondimensionalizations:

$$\tilde{U} = \frac{U}{mH}$$

$$\tilde{c} = \frac{c}{mH}$$

$$\tilde{z} = \frac{z}{H}$$

$$\tilde{\alpha}^2 = \frac{\alpha^2 H^2}{\varepsilon}$$

so that (8) and (9) become

$$\psi_{\tilde{z}\tilde{z}} + \left(\frac{r+1}{\tilde{z}-\tilde{c}} - \delta^2\right)\psi = 0 \tag{10}$$

$$\psi_{\tilde{z}} + \frac{\psi}{2} + \frac{\psi}{\tilde{c}} = 0, \quad z = 0 \tag{11a}$$

$$\lim_{z \to \infty} \psi(\tilde{z}) = 0 \tag{11b}$$

$$r = \frac{\beta H}{\varepsilon m}$$

$$\delta^2 = \tilde{\alpha}^2 + \frac{1}{4} = \tilde{k}^2 + \tilde{\ell}^2 + \frac{1}{4} . \tag{12}$$

For typical midlatitude values of constants we have

$$\beta \simeq 1.6 \times 10^{-11} \ s^{-1} \ m^{-1}$$

$$H = 8 \times 10^{3} \ m$$

$$\varepsilon = 10^{-4}$$

$$m = 1.25 \times 10^{-3} \ s^{-1}$$

$$r = 1.024$$

so that $\tilde{k}$ is related to dimensional wavelength by

$$\lambda = \frac{2\pi H}{\varepsilon}\frac{1}{\tilde{k}} = \frac{5\times10^6}{\tilde{k}}\ \text{m}. \qquad (13)$$

The twiddles are dropped in the following.

The analysis of pinch singularities outlined above requires a dispersion relation $\Delta(\omega,k)$ valid in the complex k and ω planes. In principle, the eigenproblem (10, 11) could be solved repeatedly to obtained these eigenvalues but the computational burden would be large. Fortunately, Lindzen and Rosenthal (1981) recently obtained a highly accurate WKB solution for the baroclinic problem, which is valid in the complex plane. Their dispersion relation takes the form:

$$\left\{\frac{1}{2} + \frac{k}{\omega} - \left\{\frac{1}{2x(\frac{\omega}{k})}\left(\delta^2 + \frac{r+1}{\frac{\omega}{k}}\right)^{1/2} + \frac{1}{4}\frac{r+1}{(\frac{\omega}{k})^2}\left(\delta^2 + \frac{r+1}{\frac{\omega}{k}}\right)^{-1}\right\}\right\}$$

$$\cdot \left\{-2\sin(\pi-z_T)\,e^{-i(\pi-z_T)}K_1\left(x(\frac{\omega}{k})\right) + I_1\left(x(\frac{\omega}{k})\right)\right\}$$

$$-\left(\delta^2 + \frac{r+1}{\frac{\omega}{k}}\right)^{1/2}\left\{\frac{-2\sin(\pi-z_T)}{\pi}\,e^{-i(\pi-z_T)}K_1'\left(x(\frac{\omega}{k})\right) + I_1'\left(x(\frac{\omega}{k})\right)\right\} = 0$$

where

$$z_T = \frac{\pi(r+1)}{2\delta}$$

and

$$x(\frac{\omega}{k}) = \frac{\omega}{k}\left(\frac{r+1}{\frac{\omega}{k}} + \delta^2\right)^{1/2} + \frac{r+1}{\delta}\ln\left(\sqrt{\frac{\omega/k}{r+1}}\left(\delta + \sqrt{\frac{r+1}{\omega/k} + \delta^2}\right)\right)$$

Nine term expansions of the Bessel functions were used and the real k dispersion relation obtained for a representative midlatitude value of the stability parameter r=1. The real k dispersion relation for meridional wavenumber ℓ=0 is shown in Figs.3a and 3b. Real group velocity zero can be estimated at k≃6 and k≃.7. Associated saddle points in the complex plane are shown in Fig. 4a

and, with more detail in the region near k=.7, in Fig. 4b. Contributions to the asymptotic solution for absolute instability come from these points which can be found to lie at (nondimensional) k=5.69-2.93 i, and k=.666-.113i.

The wavenumber of maximum growth predicted by normal mode analysis is k_N=1.4. Corresponding dimensional wavelength calculated from (13) are: $\lambda_N = \frac{5\times10^6}{1.4}$ m=3600 km for the normal mode and $\lambda_a = \frac{5.6\times10^6}{5.69}$ m=880 km for the absolute instability. The latter compares favorably with observed scales of cyclogenesis (Buzzi and Tibaldi, 1978; Reed, 1979).

Because these saddle points are separated in scale and arise from distinct regions of the dispersion relation — the first from the Charney mode and the second from the Burger mode, it is instructive to derive the pulse asymptotics separately. The dominant mode for any x/t can be quickly determined by comparison if desired.

Figure 5a shows the pulse shape for the saddle located in the Charney mode. Wavenumber and frequency across the pulse are shown in Fig. 5b. Note that ω_r is the rest frame frequency which is related to the local frequency by $\nu_r=\omega_r-k_r\frac{x}{t}$.

High wavenumbers are found in the vicinity of the origin of the disturbance with the leading edge of the pulse being made up of wavenumbers near the neutral point in the dispersion at k≈.87 where the real group velocity is at a maximum. Phase speeds of the short waves making up the absolute instability are small. Downstream, the wavelength rises until at the pulse peak we recover the maximum growth rate normal mode at k=1.4. Further downstream, the pulse shape is dependent on the detail of the dispersion in the neighborhood of the neutral point with the leading edge

dominated by the longest waves near k=.87. Upstream influence shows a rapid decay in space with k_i large and negative.

The pulse arising from the Burger mode is shown in Figs. 6a and 6b. The growth rate is smaller than the Charney, but nonetheless dominates the upstream influence. Upstream influence is characterized by the high negative group velocity waves and downstream by the positive with the absolute instability located near the zero of group velocity.

So far only perturbations infinite in the meridional direction, corresponding to $\ell=0$ have been considered. The saddle point method can be generalized to two or more dimensions (Bers, 1975), but these solutions present many difficulties. In fact, the initial perturbation is likely to be a distributed source of vorticity and problems associated with point sources in 2 and 3 dimensions do not necessarily yield insight commensurate with these difficulties. The simplest localized source to use is the fundamental mode in a channel, and taking this to be 5000 km wide, we choose $\ell=1/2$ in the expression for δ^2 (12). The Charney absolute instability point moves to k=5.77-2.87 i; ω=.692+.112 i, and the absolute instability point associated with the Burger mode moves to k=.516-.059 i; ω=.137+.205 i. The pulse arising from the former is shown in Fig. 7a and associated quantities in Fig. 7b. The pulse from the Burger mode is shown in Figs. 8a and 8b. We remark that the general features discussed above for the $\ell=0$ case persist, but the detail of the leading edge is modified. This effect is even more pronounced when the meridional wavenumber is further restricted to $\ell=2$, corresponding to a channel width of 1250 km. The Charney mode pulse survives and is shown in Figs. 9a and 9b. Absolute instability occurs for k=6.98-2.25 i and ω=.675+.090 i. The maximum growth rate at k=2.19 is only 1.74

times the absolute instability growth rate. What is even more remarkable is that the growth of an individual disturbance will be significantly larger than this would indicate, at least near the absolute instability point. This is because the local growth depends also on the wave phase speed in relation to the local pulse speed and the derivative of growth with local pulse speed (Simmons and Hoskins, 1979):

$$\hat{\nu}_i = \nu_i\left(\frac{x}{t}\right) + \left(c_r - \frac{x}{t}\right)\frac{\partial \nu_i}{\partial (x/t)} \,. \tag{14}$$

This effect enhances the apparent growth of wave crests between the origin and the peak of the pulse. The phase and group velocity difference is shown in Fig. 10; we can evaluate (13) for x/t=.05 to find:

$$\hat{\nu}_i \simeq .14 + (.1)(.3) = .17 \,.$$

The crest grows as fast as the maximum growth rate normal mode and with a wavenumber considerably higher being around k=4, resulting in a dimensional wavelength from (13) of λ=1250 km, which is a reasonable scale for the early stages of cyclogenesis (Reed, 1979).

2.3 Discussion and Conclusion

Absolute instability, previously found in the two-level models (but absent in the Eady problem), has been confirmed to exist in the Charney problem.

Examination of the dispersion relation for zeros of real group velocity allows a useful estimate to be made of the wavenumber characterizing the absolute instability.

Because decrease of phase speed with increasing wavenumber is a robust feature of more realistic dispersion relations (Geisler and Garcia, 1977; Simmons and Hoskins, 1976), it is suggested that the high wavenumber, low phase speed and rapid growth found for the absolute instability here may be a quite general feature.

The observation of short initial scales maturing into larger scales and possessing high growth rate encourages the identification with lee cyclogenesis (Merkine, 1977; Buzzi and Tibaldi, 1978), and at least partially answers the objection of Simmons and Hoskins (1979) that the individual low may propagate out of the region of enhanced baroclinicity before obtaining substantial amplitude.

In normal mode analysis it is generally assumed that the basic state is either zonally unbounded or periodic and a function only of height and latitude. Such uniformity is not found in the atmosphere where regions of enhanced baroclinicity result in preferred areas for cyclogenesis (Petterssen, 1956). The absolutely unstable waves described here would be able to take advantage of these inhomogeneous states by virtue of their small scale and rapid growth coupled with low phase speed. As has been noted, the predicted wavelengths of the absolute instability are commonly observed even though they are much shorter than those predicted by normal mode analysis.

The two-level and Eady models are limited by unrealistically high phase speeds, with steering levels near the center of the flow, and by the lack of a potential for zero group velocity. It would seem that the Charney problem is the simplest model that produces the observed scales.

The asymptotics of long waves which in the Charney model arise from the Burger mode were separately derived above. While the Charney mode waves in general dominate, at least in the downstream solutions, the separation in scale between the waves making up these pulses suggests that observational correlates may be found for both. In particular, the variation of the dispersion as the flow and Brunt-Vaisala frequency change, say from continental land masses to ocean or in time, may result in the absolute instability being manifest in one or the other modes separately.

It is of interest to note that amplitudes and wavelengths of long waves in the atmosphere often behave as would be expected from the above pulse asymptotics, e.g., Sanders and Gyakum (1980, their Fig. 7). Here, two areas of origin of long wave pulses may be tentatively identified: in the Atlantic off the east coast of the United States and in the Pacific near Japan.

These results imply that an accurate forecast model must closely approximate the dispersive properties of unstable waves over the entire range of wavenumbers making significant contributions to the asymptotic pulse; it is not sufficient to do well near the wavenumber of the most rapidly growing normal mode. Conversely, having an accurate local linear dispersion relation, either for the atmosphere or a model simulation, it should be possible to predict regions of cyclogenesis and the scales, phase speeds and growth rates of the unstable waves. Initially, the scale can be approximated by the wavenumber of zero group velocity.

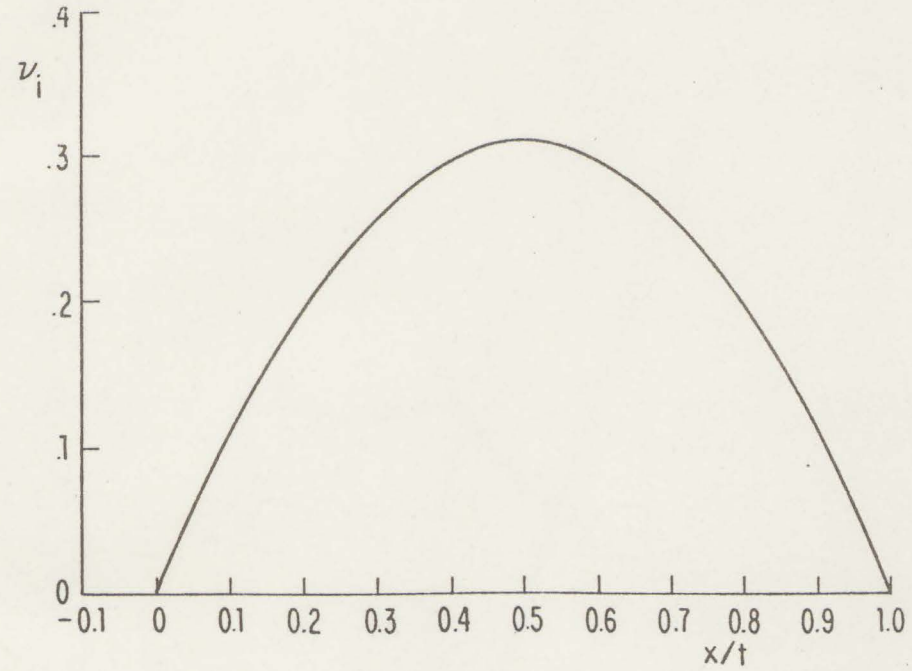

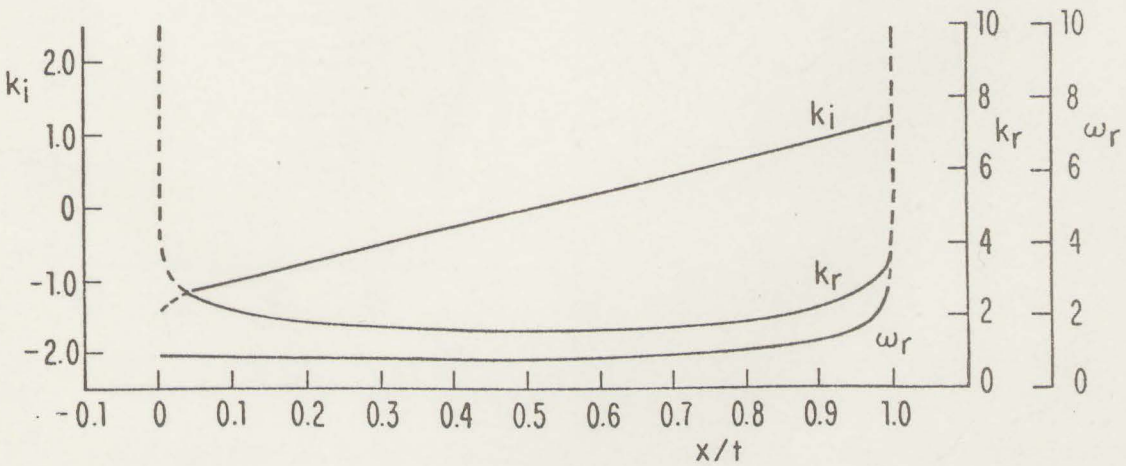

Fig. 1a Local pulse growth rate ν_i as a function of reference frame velocity x/t for the Eady example. Multiplied by any time, t_o, these axes become log of pulse amplitude as a function of distance from the origin of the disturbance.

Fig. 1b Complex wavenumbers k_r and k_i together with real rest frame frequency ω_r across the pulse in Fig. 1a.

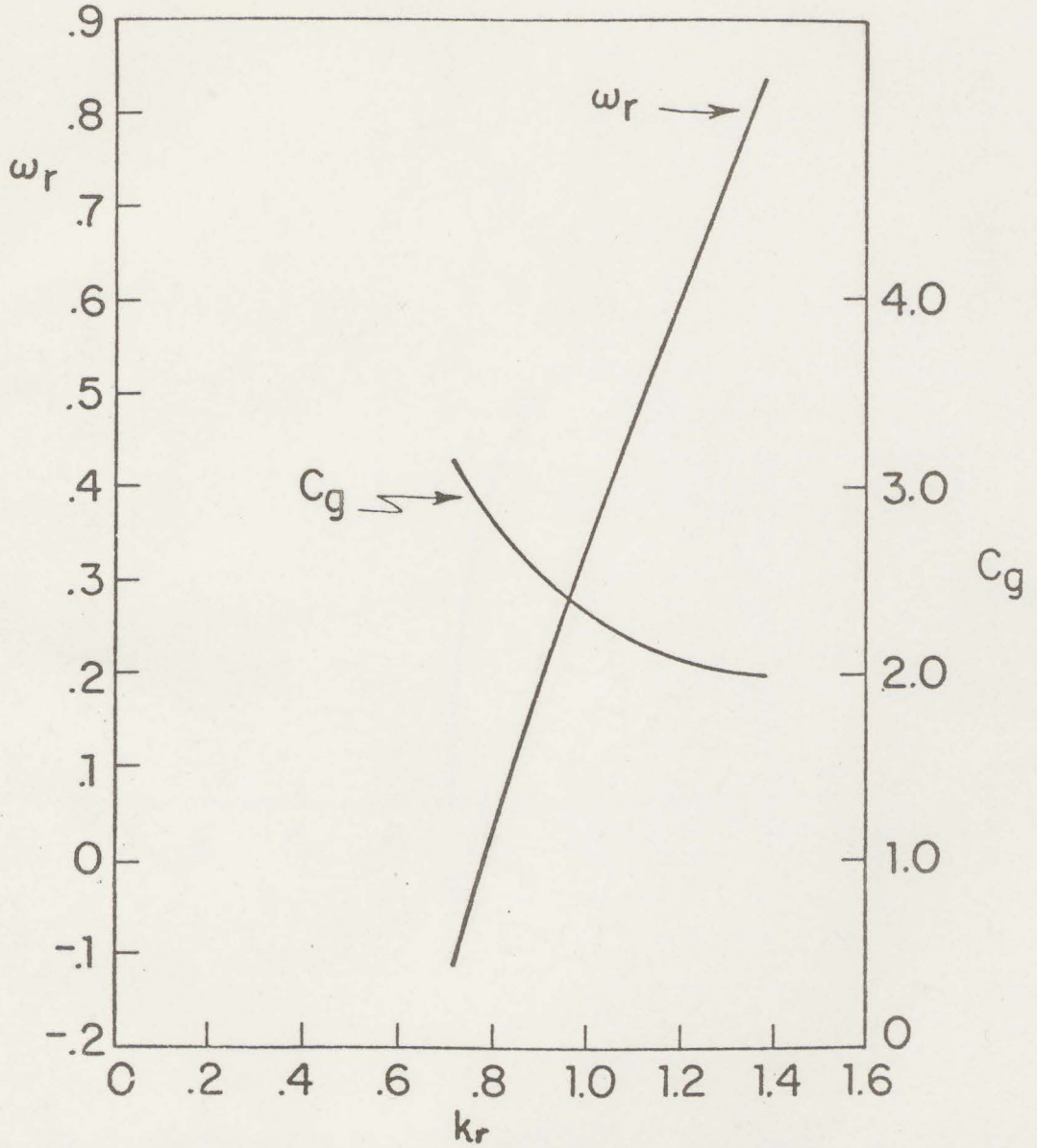

Fig 2a Nondimensional real frequency, ω_r, and group velocity, c_g, as a function of nondimensional wavenumber, k_r, for the two-level model with β=1.0 and ε=2.0.

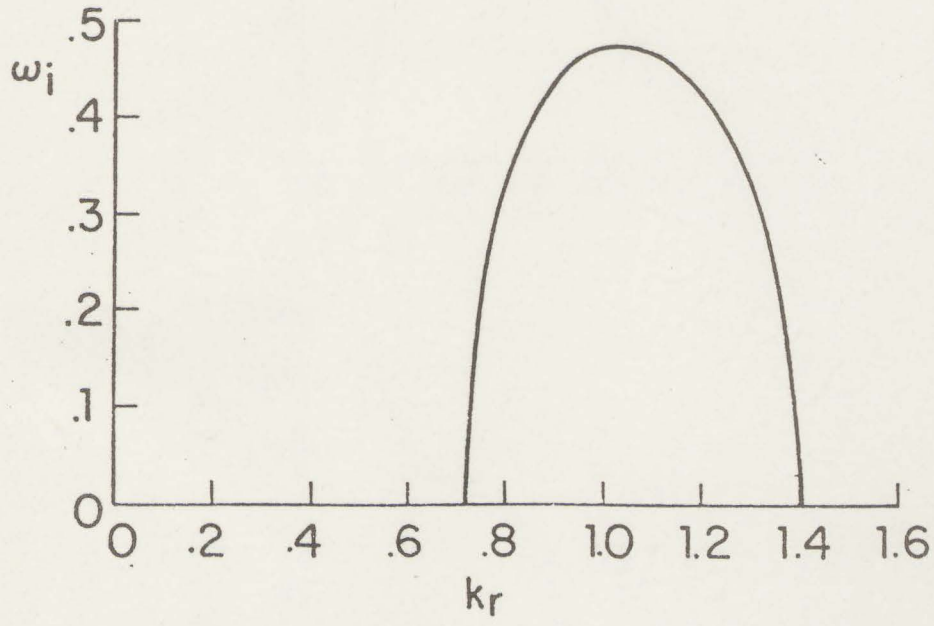

Fig 2b Growth rate, ω_i, as a function of wavenumber k_i for the example in Fig 2a.

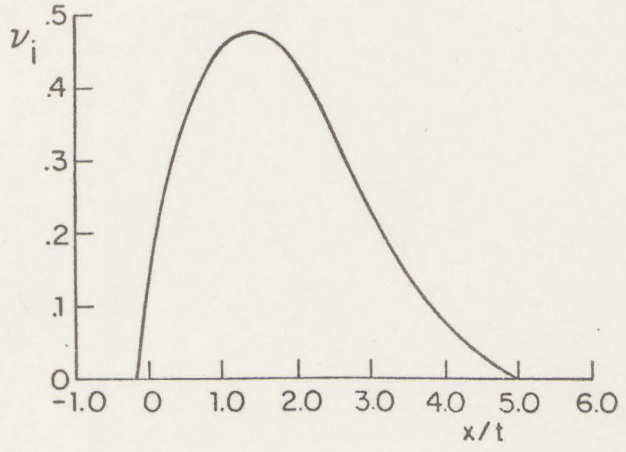

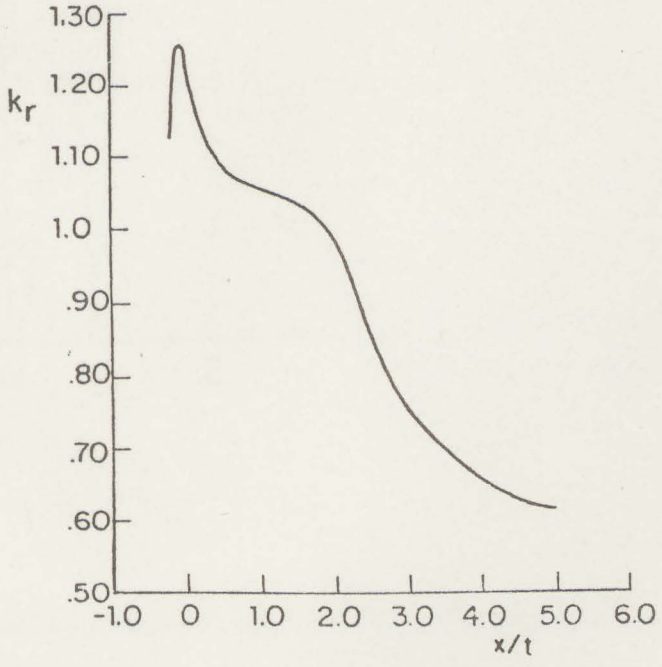

Fig 2c Local pulse growth rate, ν_i, as a function of reference frame velocity x/t for the example in Fig. 2a. Multiplied by any time, t_o, these axes become log of pulse amplitude as a function of distance from the origin of the disturbance.

Fig 2d Real wavenumber k_r across the pulse in Fig. 2c.

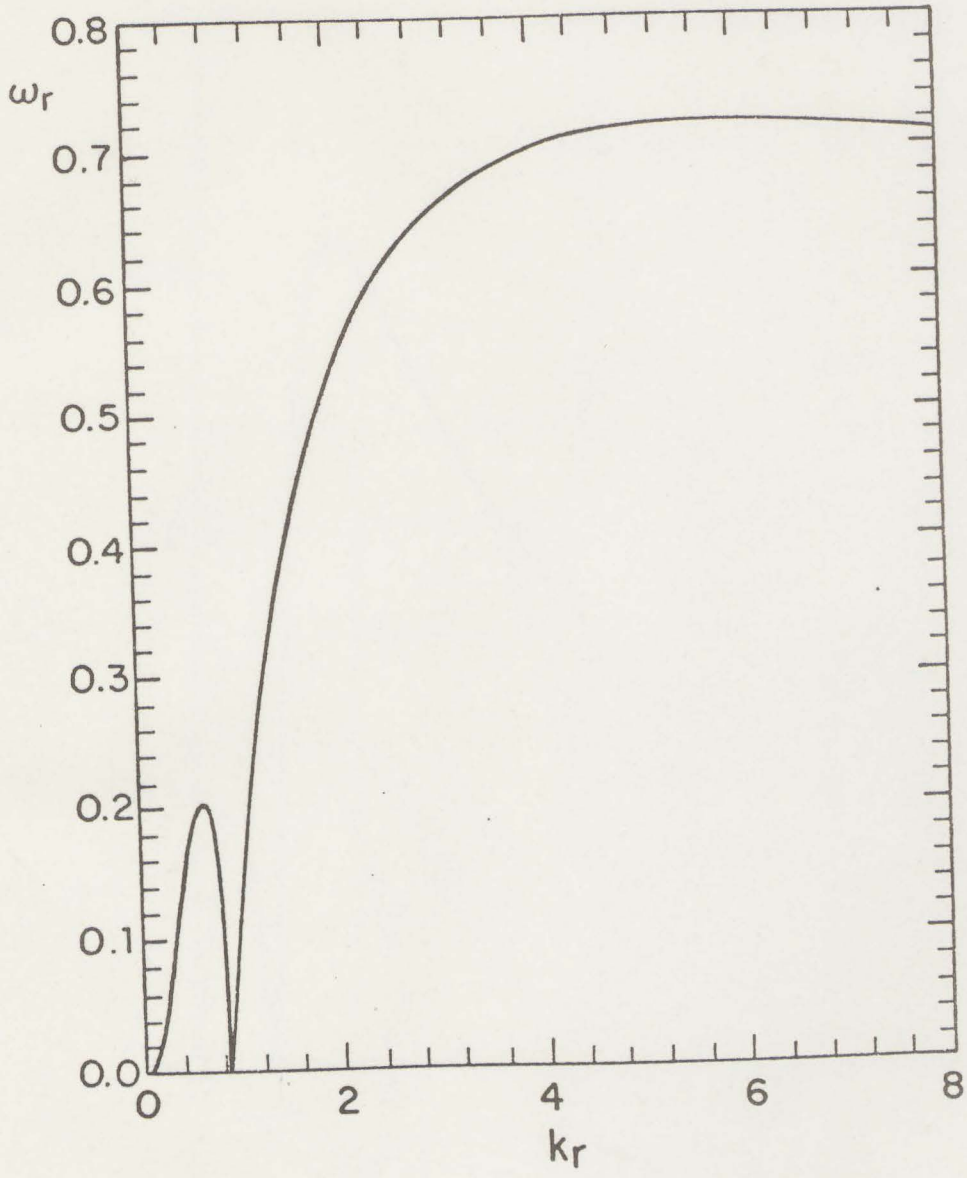

Fig. 3a. Nondimensional real frequency ω_r as a function of nondimensional real wavenumber k_r for the Charney problem with r=1.0.

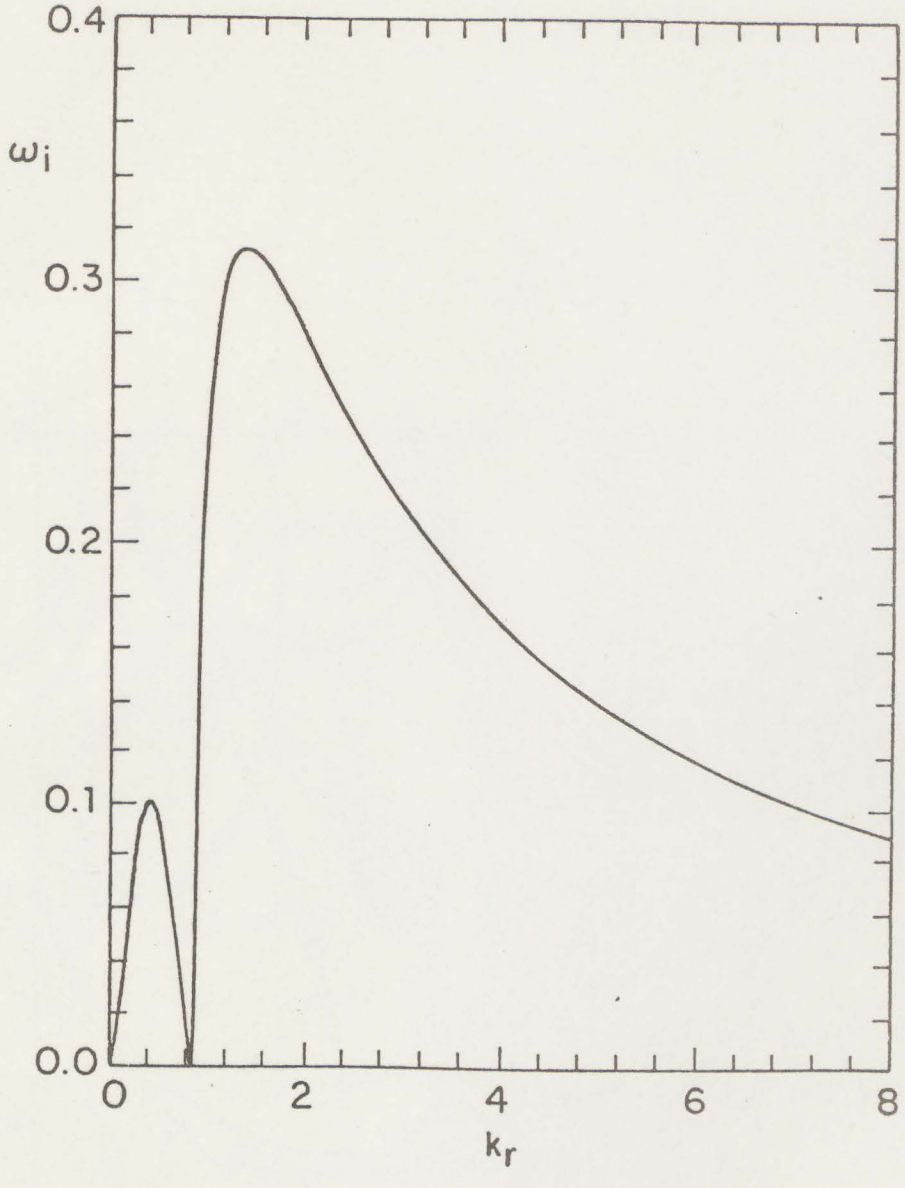

Fig. 3b. Nondimensional imaginary frequency ω_i as a function of real wavenumber k_r for r=1.0.

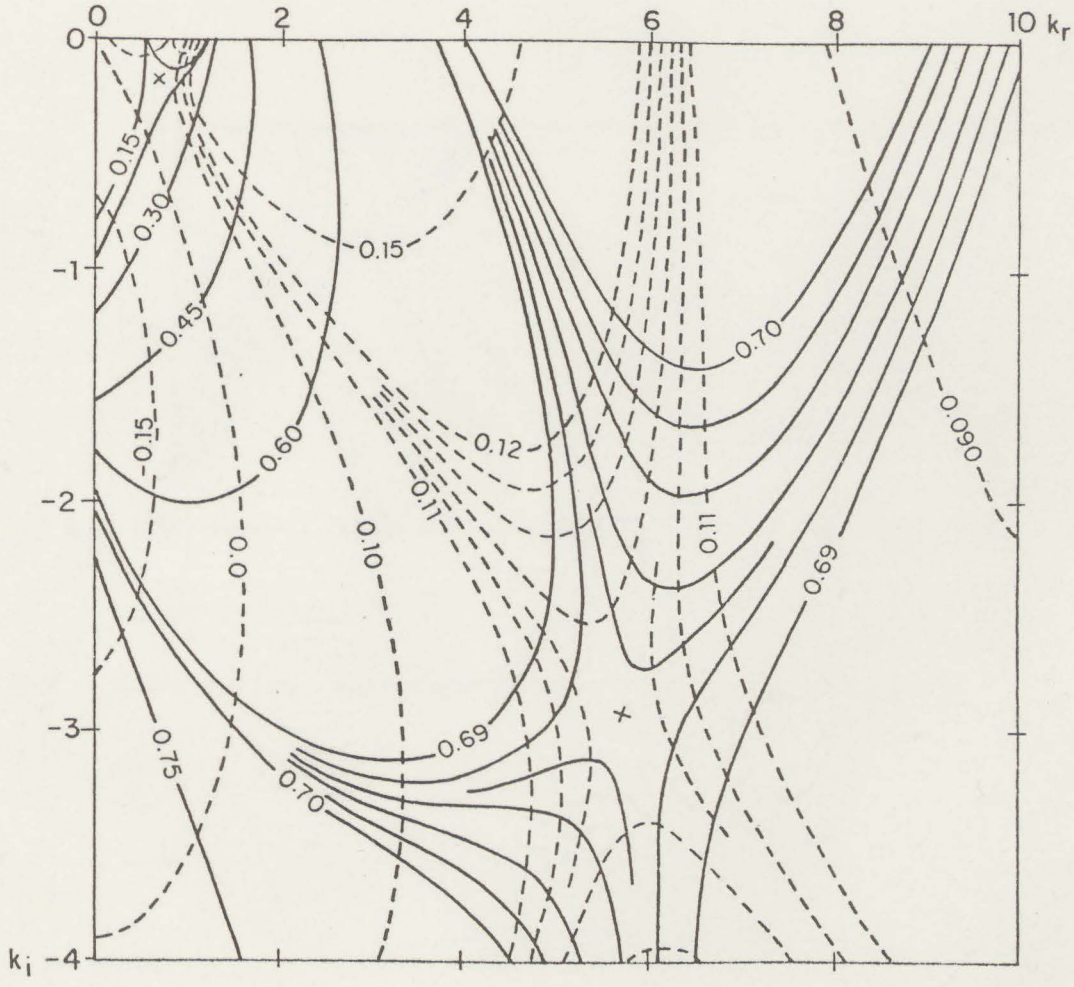

Fig 4a The complex dispersion relation for the Charney problem with ℓ=0 and r=1.0. Shown are contours of ω in the k plane. Full lines are constant ω_r, dashed lines are constant ω_i.

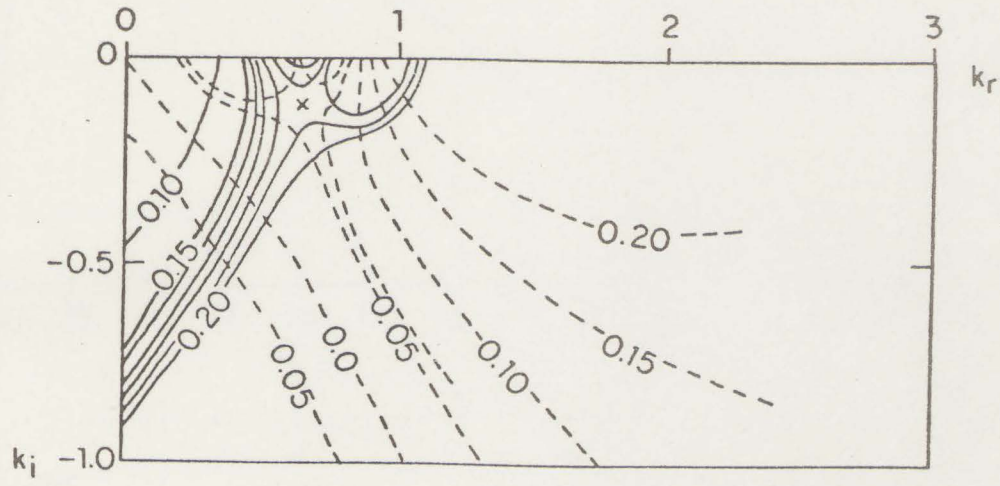

Fig. 4b Same as Fig. 4a except detail for saddle near k=.67.

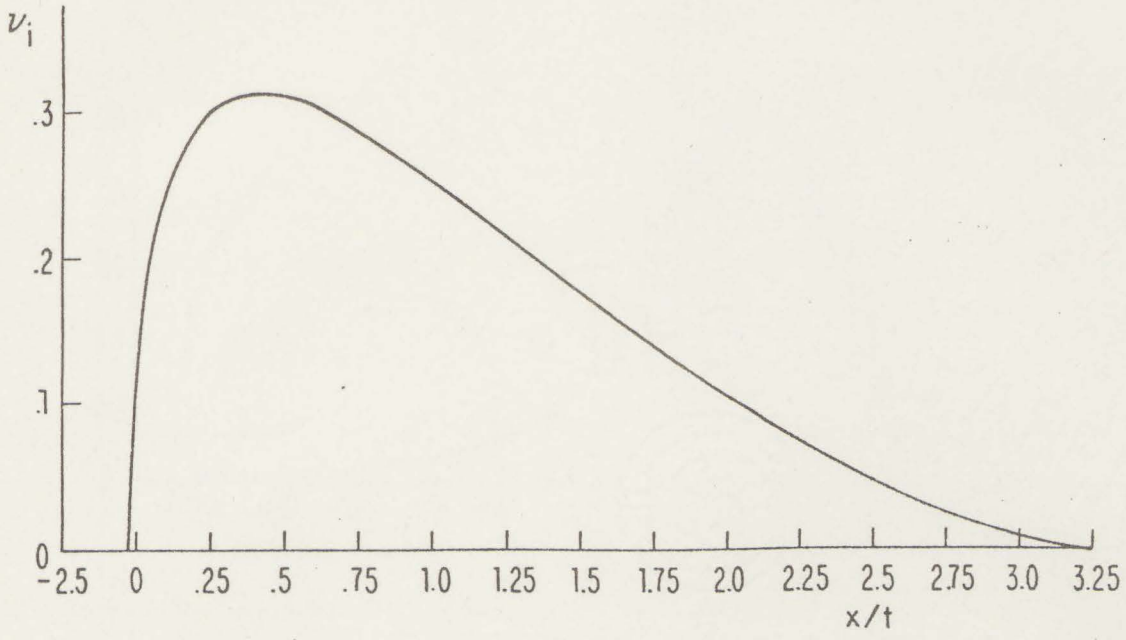

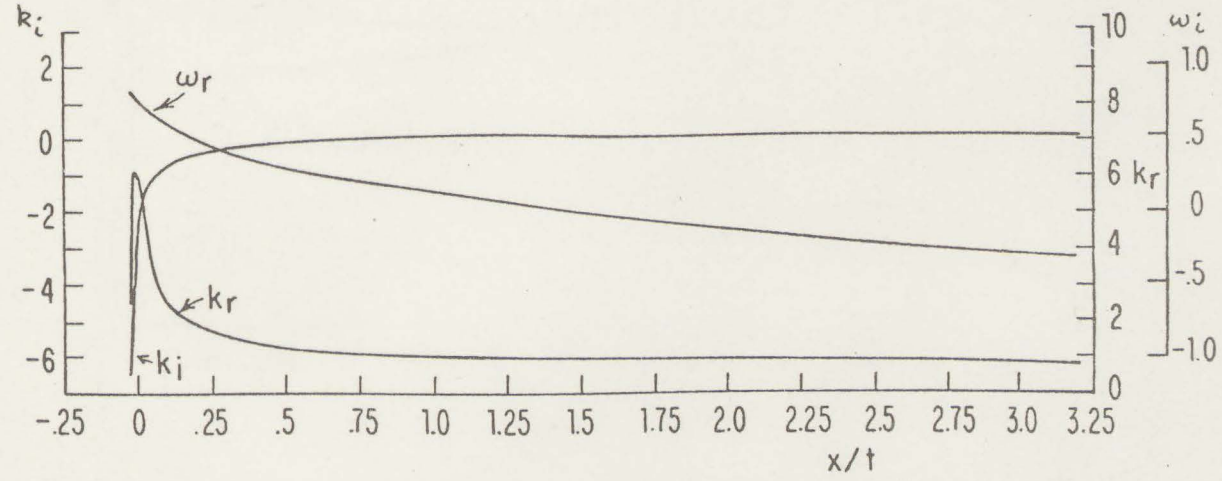

Fig 5a Local pulse growth rate ν_i arising from the saddle point in the Charney mode for ℓ=0, r=1.0, as a function of reference frame velocity x/t. Multiplied by any time, t_o, these axes become log of pulse amplitude as a function of distance from the origin of the disturbance.

Fig 5b Complex wavenumbers k_r and k_i together with real rest frame frequency ω_r across the pulse in Fig. 5a.

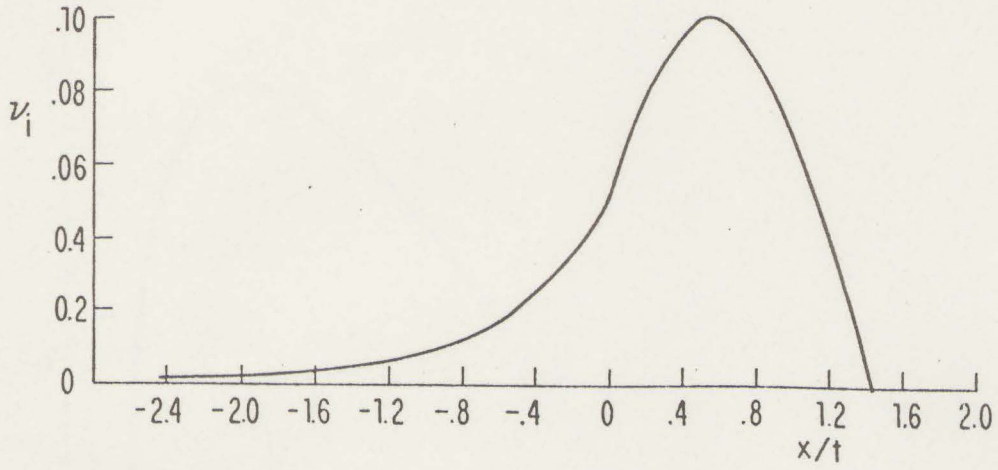

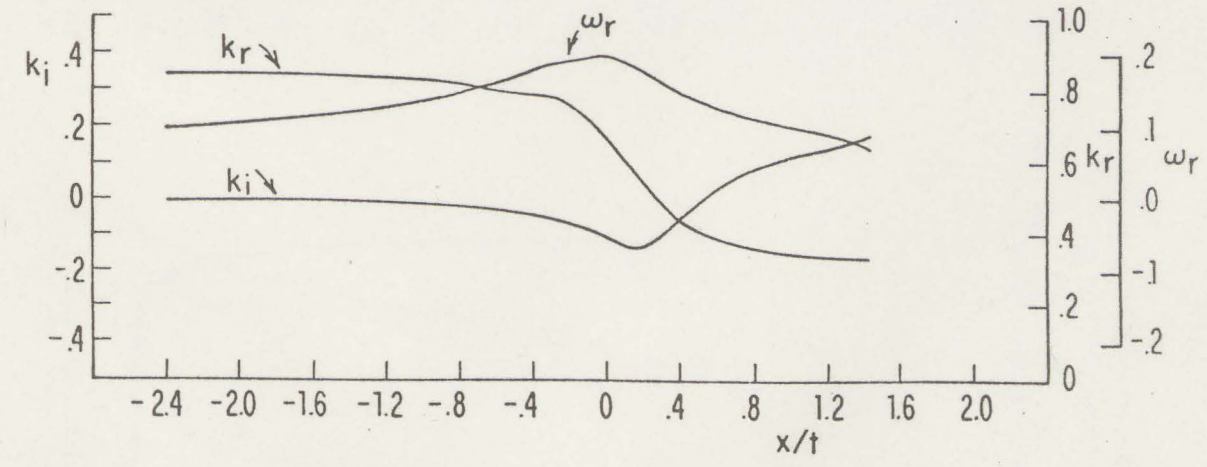

Fig. 6a Same as Fig. 5a except for the saddle point in the Burger mode.

Fig. 6b Same as Fig. 5a except for the saddle point in the Burger mode.

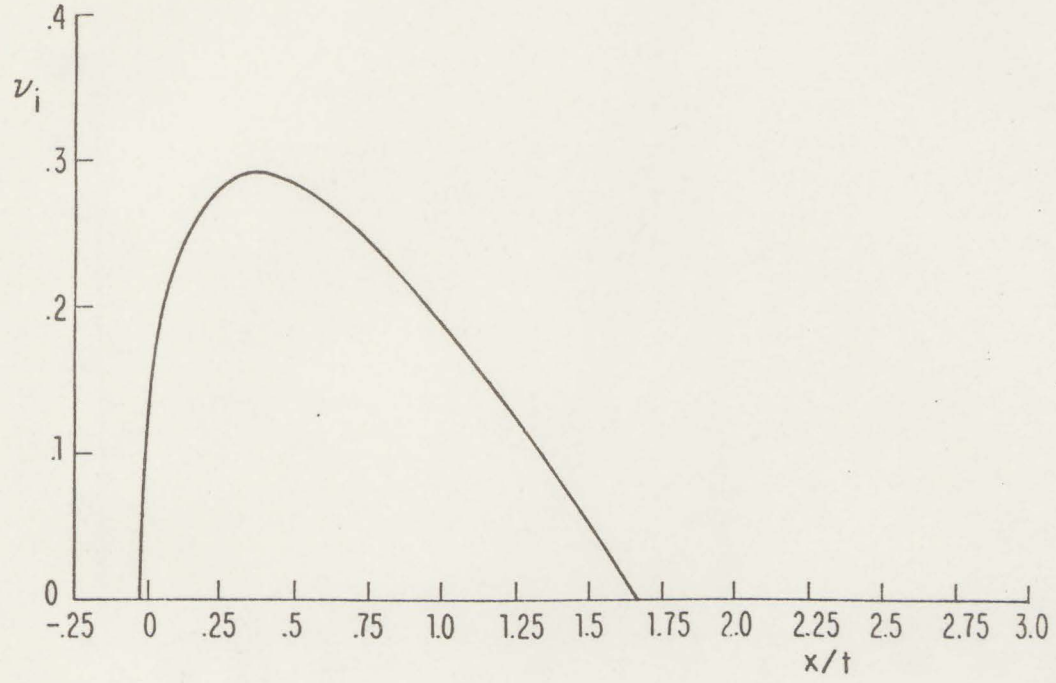

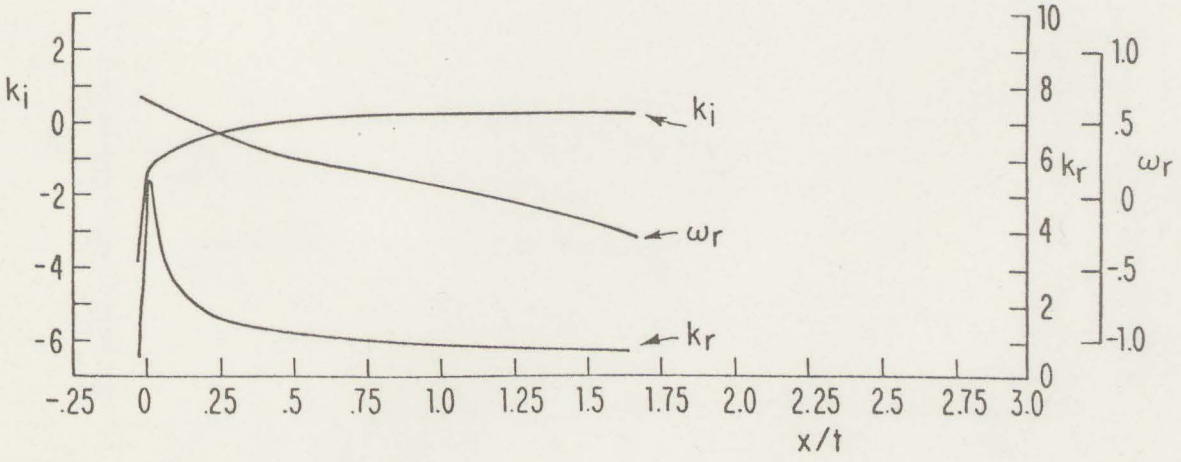

Fig. 7a Same as Fig. 5a except for $\ell=1/2$.

Fig. 7b Same as Fig. 5b except for $\ell=1/2$.

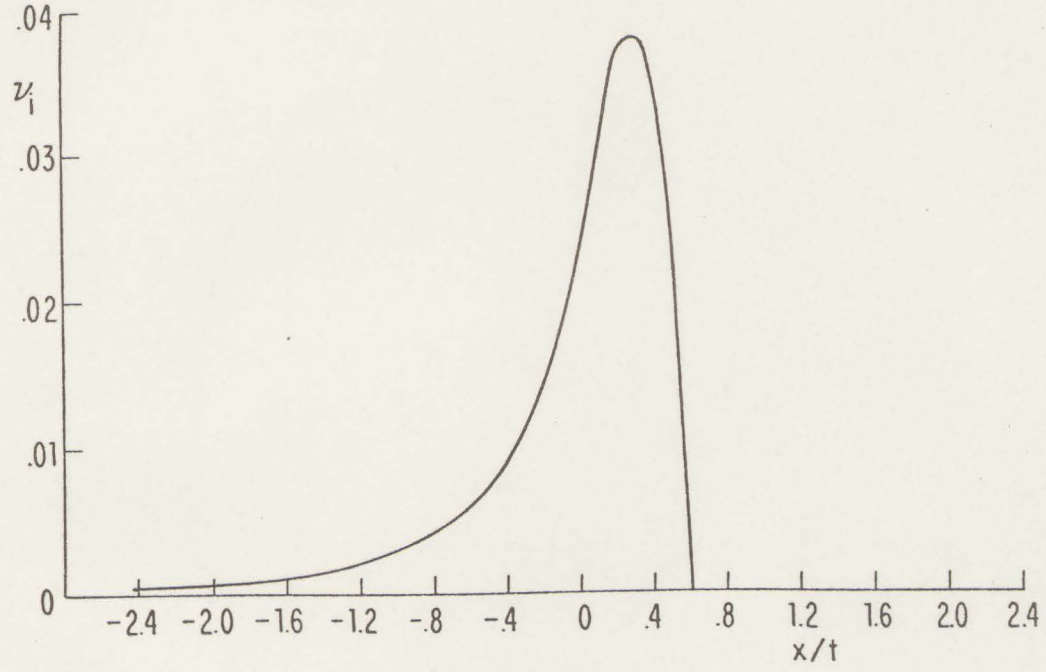

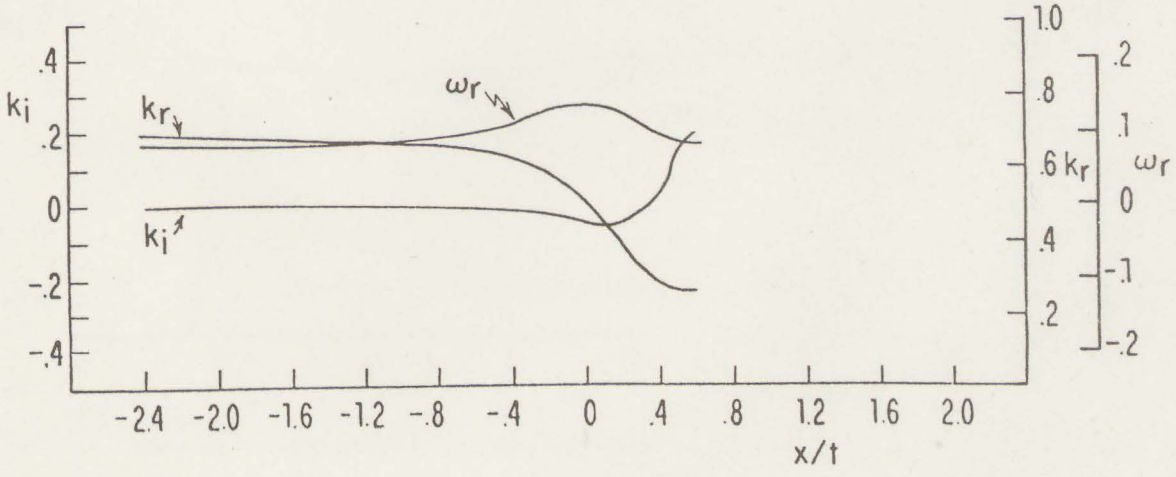

Fig. 8a. Same as Fig. 5a except for Burger mode saddle and $\ell=1/2$.

Fig. 8b Same as Fig. 5b except for Burger mode saddle and $\ell=1/2$.

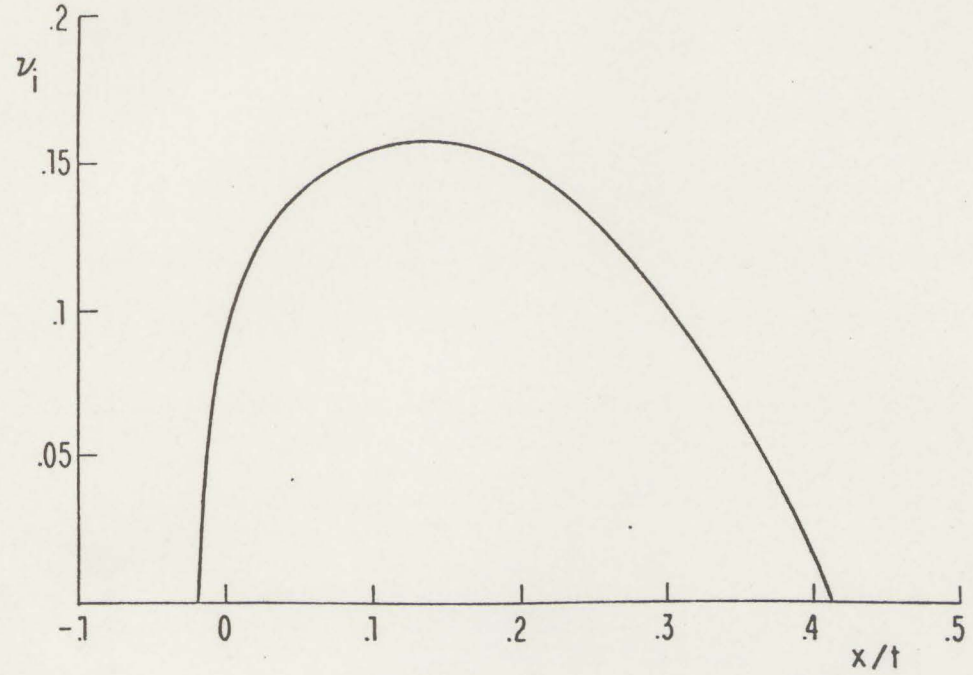

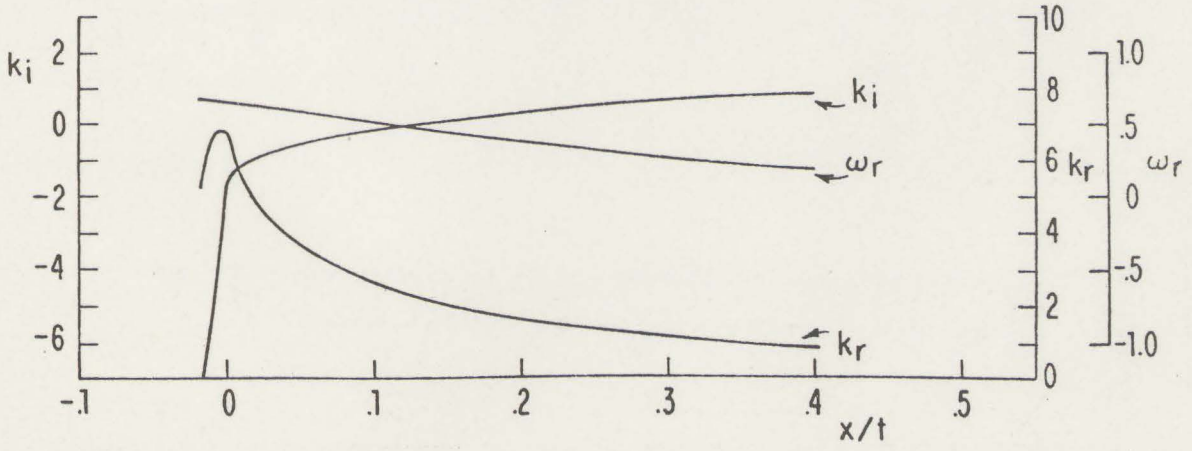

Fig. 9a Same as Fig. 5a except for ℓ=2.

Fig. 9b Same as Fig. 5b except for ℓ=2.

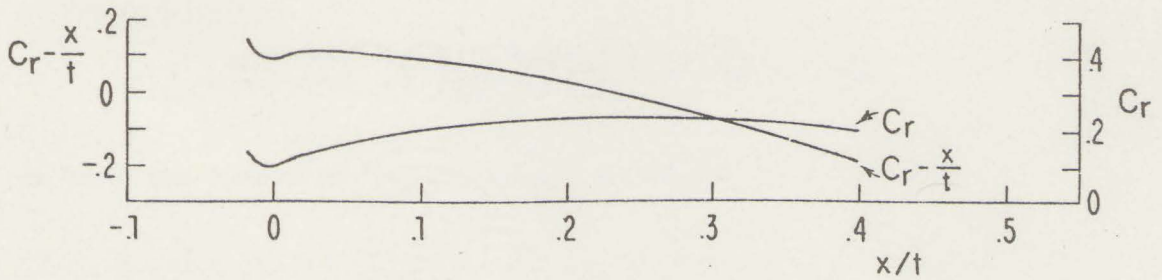

Fig. 10 Rest frame phase speed c_r and apparent phase speed as viewed from the translating frame $c_a = c_r - x/t$ for the case in Fig. 9a.

Appendix A

The dispersion relation for Eady's model can be written in the form (5):

$$\omega = \frac{k}{2} \pm i\left(k \coth k - \frac{k^2}{4} - 1\right)^{1/2}$$

$$U = \frac{1}{2}$$

$$g = \pm \left(k \coth k - \frac{k^2}{4} - 1\right)^{1/2}$$

The maximum of g, $g(k_m)=.310$, occurs at $k_m=1.6062$. (5) can be be evaluated as:

$$g^2 = k \coth k - \frac{k^2}{4} - 1$$

$$(g^2)'' = 2(g'^2+gg'') = \frac{3}{2} + 2 \coth k(k \coth^2 k - \coth k - k)$$

$$g''\big|_{km} = \frac{\frac{3}{4} + \coth k_m (k_m \coth^2 k_m - \coth k_m - k_m)}{g(k_m)} = .389$$

so that the limits of the packet are predicted to occur at:

$$\frac{x}{t} = \frac{1}{2} \pm \sqrt{2g(k_m)\left|g''\right|_{km}} = \frac{1}{2} \pm .491 > 0 ,$$

suggesting that this flow just fails to achieve absolute instability.

References

Benjamin, T. B., 1961: "The development of three-dimensional disturbances in an unstable film of liquid flowing down an inclined plane." J. Fl. Mech., 10, 401.

Bers, A., 1975: "Linear waves and instabilities." In Physique de Plasmas, C. DeWitt and J. Peyrand, Eds. New York: Gordon and Breach, 157-183.

Briggs, R. J., 1964: Electron-stream Interaction with Plasmas. Chapter 2. Cambridge: MIT Press, pp. 8-46.

Burger, A. P., 1966: "Instability associated with the continuous spectrum in a baroclinic flow." J. Atmos Sci., 23, 272-277.

Buzzi, A. and S. Tibaldi, 1978: "Cyclogenesis in the lee of the Alps: A case study." Quart. J. Roy. Meteor. Soc., 104, 271-287.

Charney, J. G., 1947: "The dynamics of long waves in a baroclinic westerly current." J. Meteor., 4, 135-162.

Eady, E. T., 1949: "Long waves and cyclone waves." Tellus, 1, 33-52.

Geisler, J. E., and R. Garcia, 1977: "Baroclinic instability at long wavelengths on a β-plane." J. Atmos. Sci., 34, 311-321.

Lindzen, R. S., Brian Farrell and Ka-Kit Tung, 1980: "The concept of wave overreflection and its application to baroclinic instability." J. Atmos. Sci., 37, 44-63.

Lindzen, R. S. and A. J. Rosenthal, 1981: "A WKB asymptotic analysis of baroclinic instability." J. Atmos. Sci., 38, 619-629.

Merkine, L.-O., 1977: "Convective and absolute instability of baroclinic eddies." Geophys. Astrophys. Fl. Dyn., 9, 129-157.

Merkine, L.-O. and M. Shafranek, 1980: "The spatial and temporal evolution of localized unstable baroclinic disturbances." Geophys. Astrophys. Fl. Dyn., 16, 175-206.

Petterrsen, S., 1956: Weather Analysis and Forecasting. Volume I. New York: McGraw-Hill, 428 pp.

Reed, R. J., 1979: "Cyclogenesis in polar air streams." Mon. Wea. Rev., 107, 38-52.

Sanders, F. and J. R. Gyakum, 1980: "Synoptic-dynamic climatology of the 'bomb'." Mon. Wea. Rev., 108, 1589-1606.

Simmons, A. J. and B. J. Hoskins, 1976: "Baroclinic instability on the sphere: Normal modes of the primitive and quasi-geostrophic equations." J. Atmos. Sci., 33, 1454-1477.

_____, 1979: "The downstream and upstream development of unstable baroclinic waves." J. Atmos. Sci., 36, 1239-1254.

Thacker, W. C., 1976: "Spatial growth of Gulf Stream meanders." Geophys. Fl. Dyn., 7, 271-295.

PART II: THE INITIAL GROWTH OF DISTRUBANCES IN A BAROCLINICALLY UNSTABLE FLOW

CHAPTER I INTRODUCTION

Since the pioneering work of Charney (1947) and Eady (1949), baroclinic instability has been accepted as a major source of propagating synoptic scale disturbances in mid-latitudes. The success of the theory in predicting approximately the scale, growth and structure of cyclone waves is by now undisputed. Results such as those of Simmons and Hoskins (1978) have extended the theory to the nonlinear regime. Observational studies have shown it to be of primary importance in atmospheric energetics and in maintenance of the observed mean flow.

The application of linear theory to explaining disturbance growth extends over most of the intensification period, although nonlinear effects are important in the mature and decay phases of cyclone life cycles, (Simmons and Hoskins, 1978). As this work is concerned with the initial growth stage, linear theory will be used throughout.

Most models,including those mentioned above have begun with the assumption of a perturbation of normal mode form or of infinitesimal amplitude so that normal mode structure prevails over the relevant time of the study. The original work of Charney and Eady cast the quasi-geostrophic equations into an eigenvalue problem and extracted only the exponentially growing and presumably negligible companion complex conjugate decaying modes. Suitably generalized to the flow in question, these were used as initial conditions in most subsequent studies. It has long been recognized (Orr, 1907, Case, 1960, Pedlosky, 1979) that the discrete normal modes do not form a complete set in the sense that an arbitrary initial condition cannot be expressed as a sum of discrete normal modes of suitably chosen amplitude. This defect was traced to the neglect of the so-called continuous

spectrum of neutral modes. These together with the discrete normal modes do in fact form a complete set for the canonical problems of Eady and Charney as was shown by Pedlosky (1964) and Burger (1966), respectively.

The careful reader may be troubled at this point by the implication that these singular neutral modes will play a key role in the development, as indeed they shall. Perhaps viscosity no matter how small would change completely the nature of the solutions. While it is true that the Navier Stokes equations support a complete set of discrete eigenfunctions and the Euler equations require a continuous infinity of singular functions for completeness, yet it appears true that predictions based on the inviscid equations are valid in the limit of vanishing viscosity even though this is a singular perturbation in the sense of the theory of differential equations. The question is examined in an exchange between Case (1960) and Lin (1961).

All flows discussed in the following will be assumed inviscid.

The method of analysis employed by Pedlosky and Burger is that of Case (1960) in which the Couette problem was cast into initial value form. The result is a combined Fourier Laplace integral for the space and time evolution of the initial perturbation. The inversion of these integrals is in general a formidable task and results were obtained for the asymptotic limit of long time only. This limit revealed not surprisingly that the exponentially growing normal mode, where present, dominated the solution. In the Couette flow where there exist no exponentially growing modes the contribution of the continuous spectrum was found to decay algebraically with time and the controversy over the order of this decay (Brown and Stewartson, (1980)) seems to have been settled in favor of Orr's original result: the streamfunction decays as t^{-2}.

The contribution of the continuous spectrum in baroclinic problems is a matter of some subtlety. In the Eady problem, Pedlosky (1964) found that for wavenumbers for which there were exponentially growing modes, the contribution asymptotically decayed but that for the neutral solutions at wavenumbers above the cutoff of exponential instability, the continuous spectrum combined with the neutral waves to give a neutral asymptotic solution. The Charney problem was shown by Burger to have a similar algebraically growing contribution associated with the continuous spectrum at the discrete neutral points and decay elsewhere where exponentially growing discrete normal modes were found.

In order to study the small time limit of the initial value problem in the most transparent manner, a major simplification will be employed: a single wavenumber in the horizontal will be used. This precludes potentially interesting interference effects arising from the Fourier inversion of Case (1960). The perturbation will be assumed to have infinite horizontal extent and a fixed wavenumber. Multiple wavenumbers which would be appropriate to localized perturbations will be only briefly considered.

To explore these ideas a simple problem for which a closed from solution exists will be examined first.

CHAPTER 2 ANALYSIS OF THE INITIAL VALUE PROBLEM

2.1 The Couette Problem

Taking $u(z)$ as the velocity profile of a plane parallel inviscid shear flow, confined between horizontal boundaries at $z = 0,1$ and $\Psi(x,z,t)$ as the perturbation streamfunction, the nondimensional, linearized equation of motion is:

$$\left(\frac{\partial}{\partial t} + u(z)\,\frac{\partial}{\partial x}\right)\nabla^2\Psi - \frac{\partial^2 u}{\partial z^2}\,\frac{\partial \Psi}{\partial x} = 0 \tag{1a}$$

$$\Psi(0) = \Psi(1) = 0 \ . \tag{1b}$$

The Couette problem results when the velocity is made linearly increasing with z: $u = z$ for which (1a) becomes:

$$\left(\frac{\partial}{\partial t} + z\,\frac{\partial}{\partial z}\right)\nabla^2\Psi = 0 \ . \tag{2}$$

Solutions are assumed of the form:

$$\Psi = \psi(z)e^{ik(x-ct)} \tag{3}$$

substituting in (2):

$$(z-c)\left\{\frac{\partial^2}{\partial z^2} - k^2\right\}\psi = 0 \ . \tag{4}$$

Eigensolutions of (4) must satisfy:

$$\frac{\partial^2 \psi}{\partial z^2} - k^2\psi = 0 \tag{5a}$$

$$\psi(0) = \psi(1) = 0 \ . \tag{5b}$$

Two linearly independent solutions of (5a) are

$$\psi_1 = \sinh kz$$

$$\psi_2 = \cosh kz \quad .$$

Of the general solution $\psi = A \sinh kz + B \cosh kz$ (5b) requires

$$B = 0$$

$$A \sinh k + B \cosh k = 0$$

which implies $A = B = 0$ so there exists no such solution.

Nevertheless it is seen by inspection that a general solution of (2) has the form for arbitrary $G(x,z)$:

$$\nabla^2\psi = G(x - zt, z) \quad . \tag{6}$$

This problem is an extreme example of the incompleteness of the eigenfunctions, having none at all. Yet it is clear from (6) that the equation is valid for any initial condition.

The resolution of this dilemma proceeds from a closer examination of (4), (Case, 1960). There are in fact two classes of solution: The above sought discrete eigenmodes, which class is empty, and solutions satisfying:

$$\left(\frac{\partial^2}{\partial z^2} - k^2\right) G(z,z_0) = \delta(z - z_0) \tag{7}$$

When the boundary condition (5b) is imposed, it is easily verified that:

$$G(z,z_0) = -\frac{\sinh kz_< \sinh k(1 - z_>)}{k \sinh k} \tag{8}$$

where:

$$z_< = \begin{cases} z & \text{if} \quad z < z_0 \\ z_0 & \text{if} \quad z \geqslant z_0 \end{cases}$$

$$z_> = \begin{cases} z & \text{if} \quad z > z_0 \\ z_0 & \text{if} \quad z \leqslant z_0 \end{cases} .$$

In this case of linear shear, the simple identification of the continuum normal mode with (8) is completed by setting

$$c = z_0 . \tag{9}$$

Using (3), the solution of (4) for initial perturbation of wavenumber k, $\Psi_{0,k}(x,z,0) = \psi_{0,k}(z)\, e^{ikx}$ is:

$$\psi_k(x,z,t) = \int_0^1 G(z,z_0) e^{ik(x-z_0 t)} \left\{ \left(\frac{\partial^2}{\partial z_0^2} - k^2 \right) \psi_{0,k}(z_0) \right\} dz_0 \tag{10}$$

which may be verified by substitution.

Using (9), (10) can be written as an integral over the normal modes:

$$\psi_k(x,z,t) = \int_0^1 G(z,c) e^{ik(x-ct)} \left\{ \left(\frac{\partial^2}{\partial c^2} - k^2 \right) \psi_{0,k}(c) \right\} dc . \tag{11}$$

For a fixed eigenvalue c, $G(z,c)$ may be interpreted as the eigenfunction and $\{(\partial^2/\partial z_0^2 - k^2)\psi_0(z_0)\}_{z_0=c}$ as the corresponding amplitude.

Assuming $\psi_{0,k}(z) = c \sin m\pi z \cos kx$ the term in curly brackets in (10) becomes $-c((m\pi)^2 + k^2)\sin m\pi z \cos kx$. Substituting this and (8) in (10), repeated integration by parts and taking the real part produces the closed form solution (Orr, 1907):

$$\psi(x,z,t) = \frac{c(k^2+(m\pi)^2)}{2k\sinh k}\Big\{[\sinh k\cos(kx+(m\pi-kt)z) - \sinh k(1-z)\cos kx - \sinh kz\cos(kx+(m\pi-kt))]/(k^2+(m\pi-kt)^2) - [\sinh k\cos(kx-(m\pi+kt)z) - \sinh k(1-z)\cos kx - \sinh kz\cos(kx-(m\pi+kt))]/(k^2+(m\pi+kt)^2)\Big\} \quad (12)$$

The long time asymptotic behavior of the stream function is $O(t^{-2})$ but the appearance of the term $(k^2+(m\pi-kt)^2)$ in the denominator suggests that for some time after an initial perturbation the disturbance may grow.

In this preliminary investigation we will concentrate on the first term in (12) so as to review what can be done by straightforward analytics. First though it is important to note a possible difficulty in interpreting the nonexponential growth of perturbations. If the amplitude of the initial perturbation in this linear problem is held fixed as the vertical wavenumber is increased in an attempt to explore the initial value problem dynamics, an ambiguity arises because the energy per unit length in x, given by

$$E = \frac{k}{4\pi}\int_0^{2\pi/k}\int_0^1 (\psi_x^2+\psi_z^2)\,dx\,dz, \quad (13)$$

increases with m. Although in problems of interest in meteorology the stream function itself represents a pressure perturbation the constancy of which may have physical justification as vertical wavenumber is changed, most results below are displayed in terms of perturbation total energy normalized by the initial total energy which shows the growth of perturbations in the most easily interpreted form.

Retaining only the first term in (12), (13) may be evaluated approximately both for $t = 0$ and for the approximate time of the maximum of (12), $t_m = m\pi/k$.

$$E(0) \simeq \frac{c^2(k^2 + (m\pi)^2)}{8k^2}$$

$$E(t_m) \simeq \frac{c^2(k^2 + (m\pi)^2)^2}{16k^4} \left\{ 1 - \frac{4(m\pi)^2}{k^2 + (2m\pi)^2} \quad \frac{\tanh k/2}{k/2} \right\}$$

The ratio:

$$\frac{E(t_m)}{E(0)} = \frac{(k^2 + (m\pi)^2)}{2k^2} \left\{ 1 - \frac{4(m\pi)^2}{(k^2 + (m\pi)^2)} \quad \frac{\tanh k/2}{k/2} \right\} \tag{14}$$

is plotted as a function of k and $m\pi$ in Fig. 1a. Note that although the plot is continuous for clarity of presentation only integer values of m satisfy the boundary condition (1b). The maximum energy occurs for longest horizontal and shortest vertical scale. An estimate of growth rate is made by dividing the maximum of energy by the time it occurs after the initial perturbation $t_m = m\pi/k$, the result is plotted in Fig. 1b. The maximum growth rate occurs for $k \simeq 3.0$.

The evolution of the streamfunction is calculated from (12) for $k = 3.0$ and $m = 6$ and the magnitude shown as a function of time Fig. 2a and Fig. 2b. Also shown in Fig. 2c is the exact normalized energy as a function of time calculated from (12) and (13) and the effective growth rate $2kc_{i\ eff} =$ $1/E\ dE/dt$, Fig. 2d.

There appear to be three stages in this growth: a relatively quiescent period immediately following the perturbation, a period of rapid growth and a period of rapid decay to the asymptotic phase where the perturbation decays as t^{-2}. Only this last stage is addressed in traditional asymptotic treatments.

Note that the rapid growth of the perturbation is coincident with a decrease in the vertical wavenumber, a phenomena that will be referred to often in the following analysis.

2.2 Discussion of the Couette Problem

As an example of the initial growth of perturbations, the Couette problem is particularly attractive because it is by far the simplest and displays much of the relevant physics. With this solution as analogy, the results to be obtained for baroclinic flows will be introduced and some preliminary comments made.

We remark first that even when linear perturbation theory predicts no instability it cannot be concluded that the flow is stable. If neutral solutions exist, then stability can only be ascertained by examining higher order terms in the perturbation expansion. Even when we are fortunate enough, as in the above example to be in possession of a complete set of modes whose integral contribution eventually decays, the amplitude of disturbance for which higher order terms may lead to instability is in general unknown. In fact the observation of small scale inflection points appearing to destabilize an otherwise stable flow in experiments (Landahl, 1975) is interesting in this regard. These observations make the fact that substantial increases in amplitude result from linear theory especially important.

In geophysical application it is often the case that modest increases in amplitude suffice to explain an observed phenomena. For example, a 5 mb initial perturbation in the geostrophic streamfunction growing by eightfold to 40 mb would be a significant deepening.

The equations describing cyclone waves are very similar to that which we have examined. Although the interpretation of terms is different, a parallel phenomena is seen and even when exponentially growing modes are

present, the initial growth can dominate the solution over relevant time scales, that is, the normal mode structure develops only after significant growth has occurred by this alternate mechanism.

Returning to the example of parallel flow of an inviscid fluid, an energy integral may be obtained in the standard way:

$$\frac{d}{dt}\int_0^1 \frac{1}{2}\left(\overline{\psi_x^2} + \overline{\psi_z^2}\right) dz = \int_0^1 \bar{U}_z \overline{\psi_x \psi_z}\, dz \qquad (15)$$

where

$$(\bar{\ }) = \min_{x\to\infty} \int_{-x}^{x} (\ )\, dx \quad .$$

This relates the increase in disturbance energy to the work done on the perturbations by the Reynolds stress. Parallel expressions exist for baroclinic and barotropic flows (Pedlosky, 1979). While no normal modes exist for which the relative phase of the vertical and horizontal velocity is such as to render the RHS of (15) positive, an initial perturbation may have this property or as happened in the above may acquire it by virtue of being sheared by the basic state flow. (Incidently, this explains the slow initial phase growth in the above solution (Fig. 2d); ψ_x and ψ_z are initially in quadrature.) This phenomena is familiar to students of meteorology from the work of Pedlosky (1979), whose small amplitude waves continue to grow through a large part of the vacillation cycle after the nonlinear terms have stabilized the flow to normal mode perturbations. This occurs because the disturbances are still in possession of relative phases which result in their extracting energy from the mean flow. If by a

conspiracy of intent the initial condition were of this form the same solution would of course be found even though the flow was not initially unstable.

The energy integral (15) places an upper bound on the growth rate of perturbations. From (15) :

$$\frac{dE}{dt} = \frac{d}{dt}\int_0^1 \frac{1}{2}\left(\overline{\psi_x^2} + \overline{\psi_z^2}\right) dz \leq |\overline{U}_z|_{max} \int_0^1 |\overline{\psi}_x||\overline{\psi}_z| \, dz$$

which together with the inequality:

$$\overline{\psi}_x^2 + \overline{\psi}_z^2 \geq 2\,|\overline{\psi}_x||\overline{\psi}_z|$$

gives:

$$\frac{1}{E}\frac{dE}{dt} \leq |\overline{U}_z|_{max}$$

The example in Fig. 2d obtains ~ 70 percent of this maximum.

The inviscid incompressible Navier Stokes equations in two dimensions possess two independent integral invariants: energy and enstrophy which is the integrated square vorticity. The conservation of energy is familiar and the equations are often written as to explicitly display the conservation of vorticity. Vorticity is conserved point by point so any other function of vorticity when integrated over the domain of flow, is also a conserved quantity but is not an independent invariant. In the case of quasi-geostrophic flow, the energy and pseudopotential vorticity are the parallel conserved qnatities (Charney, 1973). The reader is cautioned that these quantities are conserved by the complete equations, however, the linearized equations can be closed by including the second order corrections to the mean flow (Pedlosky, 1979). If the evolution of an

initial disturbance is viewed as the trajectory of a point in a suitably defined phase space, then the integral invariants limit this trajectory to surfaces which satisfy energy and vorticity conservation. These constraints potentially limit the extent to which a perturbation to a basic state may grow. For the case of parallel flows the following can be shown by integral techniques to hold for small perturbation (Arnold, 1965).

$$\frac{d}{dt} \int (\nabla\psi)^2 + \frac{\nabla\Psi}{\nabla\Delta\Psi} (\Delta\psi)^2 \, dv = 0 \qquad (16)$$

$\psi = \psi(x,z,t)$ = perturbation streamfunction

$\Psi = \Psi(z)$ = streamfunction of the basic state.

In our examples, $\frac{\nabla\Psi}{\nabla\Delta\Psi} = \frac{U(z)}{U''(z)}$ so that (16) may be written:

$$\frac{d}{dt} \int (\nabla\psi)^2 + \frac{U}{U''} (\Delta\psi)^2 \, dv = 0 \quad . \qquad (17)$$

The Rayleigh and Fjortoft theorems (Charney, 1973) are immediate consequences of (16) as a change in sign of:

$$F(z) = \frac{U}{U''} \qquad (18)$$

in the domain of flow allows arbitrary growth.

Concentrating on the case of stable flows with $U/U'' > 0$ it can be seen that (17) permits the energy of the perturbation to grow at the expense of the enstrophy. Furthermore, the extent to which a change in enstrophy is able to be traded for increased energy is governed by the term U/U''.

For these problems, the stability is not affected by the addition of a uniform velocity to the basic state, U. The choice resulting in the tightest bound from (17) is preferred. For instance, Fjortoft's theorem results when $U = 0$ is coincident with the inflection point $U'' = 0$.

As an example, the basic state:

$$U(z) = z + \frac{\varepsilon z^2}{2}$$

gives for (18):

$$F(z) = \frac{z + \frac{\varepsilon z^2}{2}}{\varepsilon} \tag{19}$$

which for $\varepsilon \to 0$ allows arbitrary large increases in energy for a decrease in enstrophy. Note that this limit corresponds to the Couette problem. Indeed it is easily verified by inspection of (2) that despite the change in vertical wavenumber and energy entailed in the examples above, the enstrophy remains constant. If $F(z)$ is viewed as an indication of the potential of a basic state to exhibit initial value growth then the Couette problem at first glance appears to have unlimited potential. For other basic states the bound is tighter as can be seen by allowing ε large in (19). The Couette problem is exceptional in the sense that (16) fails to provide a tight bound on the growth of perturbations. A much better bound can be obtained (Appendix A).

Of course, there is no guarantee that the detailed dynamics of a perturbation will give rise to a decrease in enstrophy and concomitant increase in energy, but this is usually observed for high enstrophy initial conditions.

If the vertical wavenumber is large, there is potential for great energy growth even for modest values of $F(z)$ as can be seen by noting that the ratio of enstrophy to energy for $\psi(z) \sim \sin mz$ is:

$$\frac{(\Delta\psi)^2}{(\nabla\psi)^2} \cong m^2 \quad .$$

Although (16) gives no bound in the case of unstable flows for which $F(z)$ changes sign in the domain, the initial value growth mechanism continues to operate as will be shown by examples to follow. In fact, low vertical wavenumber normal modes whether neutral or unstable appear to be efficiently produced by this mechanism resulting in initial growth rates much higher than would be expected from an examination of their eigenvalues. It is important to note in this connection that these discrete and continuous normal modes have no orthogonality properties so that no result of the kind expressed in Parseval's theorem (Jeffreys and Jeffreys, 1972) exists. Because of this, it is possible for a high amplitude discrete normal mode to be present in the expansion of a small initial perturbation, only to be revealed when the continuous spectrum decays away.

2.3 Baroclinic Initial Value Problems

The behavior of small perturbations to a baroclinic fluid in zonal flow is governed by the linearized equation expressing the conservation of pseudo potential vorticity (Pedlosky, 1979):

$$\left(\frac{\partial}{\partial t} + U\frac{\partial}{\partial x}\right) q + \frac{\partial \psi}{\partial x}\frac{\partial \Pi}{\partial y} = 0 \qquad (20a)$$

with boundary condition requiring the vertical velocity to vanish on rigid horizontal surfaces:

$$\left(\frac{\partial}{\partial t} + U\frac{\partial}{\partial x}\right)\frac{\partial \psi}{\partial z} - \frac{\partial U}{\partial z}\frac{\partial \psi}{\partial x} = 0 \qquad z = 0,\ z_T \qquad (20b)$$

where:

x = eastward coordinate

y = northward coordinate

z = height

$U(z)$ = basic state zonal velocity

ψ = perturbation geostrophic streamfunction

$q = \nabla^2\psi + \frac{1}{\rho\varepsilon}\frac{\partial}{\partial z}\left(\varepsilon\rho\ \frac{\partial \psi}{\partial z}\right)$ = perturbation potential vorticity

$\varepsilon = \frac{f^2}{N^2}$ square ratio of the Coriolis parameter to the Brunt-Vaisala frequency

ρ = density

$\Pi_y = \beta - \frac{\partial^2 U}{\partial y^2} - \frac{1}{\rho\varepsilon_s}\frac{\partial}{\partial z}\left(\varepsilon\rho_s\frac{\partial U}{\partial z}\right)$ meridional gradient of potential vorticity of the basic state.

$\beta = \frac{\partial f}{\partial y}$

Notice that (20) is made to correspond to (1) except for the boundary condition:

$$\psi_z(0) = \psi_z(z_T) = 0$$

by considering the boundary as a δ-function in π_y (Bretherton, 1966; Lindzen et al., 1980); this is accomplished by bending the velocity profile $U(z)$ in the immediate vicinity of the boundary so that $U_z = 0$, $z = 0$, z_T.

The energy integral for the y-independent perturbations is:

$$\frac{dE}{dt} = \frac{d}{dt}\int_0^{z_T} \frac{\rho}{2}\left[\overline{(\psi_x)^2} + \varepsilon\overline{(\psi_z)^2}\right] dz = \int_0^{z_T} \rho\varepsilon \frac{\partial U}{\partial z}\,\overline{\frac{\partial \psi}{\partial x}\frac{\partial \psi}{\partial z}}\, dz \qquad (21)$$

Comparing with (15) the structure of the equation is the same but the terms on the LHS are interpreted as kinetic and potential energy respectively while the source on the RHS is heat flux down the global temperature gradient. It is expected that an initial perturbation which results in the RHS of (21) being positive or which obtains this correlation under the action of the basic state shear will exhibit initial growth.

The energy integral (21) places an upper bound on the growth rate of perturbations in parallel with that derived in section 3 for the inviscid shear flow:

$$\frac{1}{E}\frac{dE}{dt} \leq \left|\sqrt{\varepsilon}\, U_z\right|_{max}.$$

This bound is approached in examples to follow.

Arnol'd's result has been generalized to quasi-geostrophic flows (Blumen, 1968). The twin constraints of energy and potential vorticity conservation require that perturbation energy and enstrophy be related as the disturbance evolves by:

$$\frac{d}{dt}\left\{\int_0^{z_T} \rho(\overline{\psi_x^2} + \varepsilon\overline{\psi_z^2}) - \frac{U(z)}{\beta - \frac{1}{\rho\varepsilon}\frac{\partial}{\partial z}\left(\rho\varepsilon\frac{\partial U}{\partial z}\right)}\overline{q^2}\, dz\right\} = 0 \qquad (22)$$

where the boundary terms have been absorbed by bending $U(z)$ so $U_z = 0$ at the boundaries and the β-plane approximation has been made.

The criterion for stability:

$$F(z) = \frac{-U(z)}{\beta - \frac{1}{\rho\varepsilon}\frac{\partial}{\partial z}\left(\rho\varepsilon\frac{\partial U}{\partial z}\right)} > 0$$

implies for an exponentially stratified atmosphere, $\rho = \rho_0 e^{-z/H}$, with ε constant that:

$$\frac{-U(z)}{\beta + \frac{U_z}{H} - U_{zz}} > 0 \quad .$$

The fluid is potentially unstable unless $\beta + \frac{U_z}{H} - U_{zz}$ is of one sign, in which case $F(z) > 0$ and the initial growth mechanism would allow the energy of perturbations to grow as described above; whether the potential growth is realized would have to be determined by solving (20) for any particular initial condition.

The flow may be stabilized to exponentially growing disturbances by modifying $U(z)$ so that the Rayleigh stability criterion is satisfied (Lindzen et al., 1980):

$$\Pi_y = \beta + \frac{U_z}{H} - U_{zz} \geq 0 \qquad 0 \leq z \leq z_T \quad .$$

In this case $F(z) > 0$.

In summary, we will show that baroclinic flows can exhibit growth of an initial perturbation whether the flow has been stabilized to exponential perturbations or not. The growth is limited by this integral constraint only for the exceptional cases of $F(z) > 0$.

2.4 Preliminary Discussion of Baroclinic Initial Value Examples

The canonical examples of baroclinic instability for the quasi-geostrophic equations are the solutions of Charney (1949) and Eady (1949). These have been shown to possess a complete set of normal modes when the discrete normal modes (there are two for every horizontal wavenumber except for isolated neutral points in the Charney problem) are augmented by the continuum of neutral modes (Pedlosky, 1964 , Burger, 1966). The solution is found in terms of a Laplace transform of the relevant Greens function in the manner of Case (1960) who used this formalism for the Couette problem. The initial value problem is solved by inversion of these transforms. Unfortunately, the Greens functions, while simply expressed in terms of the solutions of the equation, result in cumbersome Laplace inversions. Initial value results were confined in the above mentioned investigations to the long time asymptotics which show the familiar discrete normal mode spectra and decay of the continuum contribution except for the Eady neutral waves where a component of the continuous spectrum combines with the neutral discrete normal modes to produce an O(1) asymptotic contribution and the isolated neutral points of the Charney problem where the continuum contribution grows O(t).

The initial growth of perturbations could in principle be found by inverting numerically the Laplace transform but this approach presents many difficulties. Instead, the results to be presented below were derived by integrating the equations for different initial conditions. The method employed (Appendix B) was to assume normal mode solutions:

$$\psi_N(x,z,t) = \psi_N(z)e^{ik(x-c_N t)} \tag{23}$$

and finite difference (20) in z. The resulting matrix was then resolved into normal modes, ψ_N, using the highly efficient QR algorithm (Wilkinson, 1965).

An initial perturbation can be projected on these normal modes and the streamfunction $\theta(x,z,t)$ at later time found by summing over (23):

$$\theta(x,z,t) = \sum_N a_N \psi_N(z) e^{ik(x-c_N t)} \tag{24}$$

where

$\psi_N(z)$ = N'th normal mode

c_N = complex phase speed of N'th normal mode

a_N = projection of initial condition on $\psi_N(z)$.

The advantage of this method is that once the eigenvectors and eigenvalues have been extracted for a given horizontal wavenumber k, the integration for various initial conditions requires little computational effort. In addition, the projection of the initial condition on the discrete normal modes immediately reveals to what extent they are excited. The fact that the complete set of normal modes, while independent, are not orthogonal allows the amplitude of initial excitation of exponentially growing modes to be large for a relatively modest initial disturbance.

The disadvantage of the method is that it requires the approximation of the continuum spectrum by a finite number of modes, or equivalently the approximation of the continuous atmosphere by a finite number of levels (Pedlosky, 1979). Experience shows that accurate solutions for vertical wavenumber four perturbations require no more than 50 levels although as many as 150 levels have been used to check accuracy.

2.5 The Eady Problem

The Eady problem results when (20) is restricted to $\beta = 0$, N constant, the Bousinesq approximation is made, the shear assumed linear ($U(z) = z$), and horizontal boundaries are imposed at $z = 0,1$:

$$(\tilde{z} - \tilde{c})\left(\frac{\partial^2 \psi}{\partial \tilde{z}^2} - \tilde{k}^2 \psi\right) = 0 \tag{25a}$$

$$(\tilde{z} - \tilde{c})\psi_{\tilde{z}} - \psi = 0 \qquad \tilde{z} = 0,1 \tag{25b}$$

where solutions for infinite meridional scale of the form $\psi(x,z,t) = \psi(z)e^{ik(x-ct)}$ have been assumed and the following nondimensionalization made:

$\tilde{k} = \frac{kH}{\sqrt{\varepsilon}}$ nondimensional horizontal wavenumber

$\tilde{z} = z/H$ nondimensional height

$\tilde{t} = t \wedge \sqrt{\varepsilon}$ nondimensional time

H = scale height

$\varepsilon = \frac{f^2}{N^2}$

f = Coriolis parameter

N = Brunt-Vaisala frequency

$\Lambda = \frac{\partial U}{\partial z}$ shear of mean flow, assumed constant.

For reference we note typical mid-latitude values of constants:

$\beta = 1.6 \times 10^{-11}\ s^{-1}m^{-1}$

$H = 8 \times 10^3\ m$

$$f = 10^{-4}\ s^{-1}$$

$$N = 10^{-2}\ s^{-1}$$

$$\Lambda = 1.25 \times 10^{-3}\ s^{-1}$$

so that $\tilde{k}$ is related to dimensional wavelength by:

$$\lambda = \frac{H}{\sqrt{\varepsilon}} \frac{2\pi}{\tilde{k}} = \frac{5 \times 10^{6}\ m}{\tilde{k}} \tag{26}$$

and $\tilde{t}$ is related to dimensional time by:

$$t = \frac{\tilde{t}}{\Lambda\sqrt{\varepsilon}} = 22\tilde{t}\ \text{hrs} \quad . \tag{27}$$

It is important to note in evaluating quantities which are functions of $\tilde{t}$ that a unit of nondimensional time is related to dimensional time by the inverse shear. Here we have assumed a 10 ms^{-1} zonal velocity at 8 km resulting in a 22 hr $\tilde{t}$, but three or even four times this may be appropriate to strong jets resulting in a 6-8 hr $\tilde{t}$.

Twiddles will be dropped in the following.

The eigenvalues of the discrete normal modes are shown in Fig. 3a. There are two such modes at each value of the horizontal wavenumber, k. For $0 < k < 2.39994$ these correspond to complex conjugate modes, one growing and one decaying; for $k > 2.3994$ there are two neutral waves. The maximum growth rate occurs for $k_m = 1.6062$. Normal mode structure at k_m is shown in Fig. 3b along with an example of the continuous spectrum at $c = .7$. Figure 3c shows the normal mode structure at $k = 3.0$, in the region of neutral discrete normal modes.

Because the long time asymptotic limit of an exponentially unstable wave has an energy growth $E(t)/E(0) = e^{2kc_i t}$, the results of initial value integrations for unstable waves will be displayed by plotting the instantaneous growth rate:

$$2kc_{i_{eff}} = \frac{1}{E}\frac{dE}{dt} \quad .$$

Integrations were performed for $k = k_m$ and initial perturbations vertical wavenumbers, $\ell = m\pi$, $m = 0,2,4,8$. The growth rate as a function of time is shown in Fig. 4. Associated streamfunctions are also shown, Fig. 5. Similar integrations for $k = 2.3$, where an exponentially unstable normal mode of lower growth rate is found were performed with the results in Figs. 6 and 7. The region of neutral discrete normal modes at $k = 2.4$ yields the results in Figs. 8 and 9, and $k = 3.0$ the results in Figs. 10 and 11.

We are fortunate in the case of the Eady problem in that there exists a solution for arbitrary k and $m = 0$ in terms of a definite integral which is easily evaluated numerically (Simmons and Hoskins, 1979). Solutions generated for $m = 0$ by the matrix method described above were found to agree with this independent solution.

2.6 Discussion of Eady Solutions

For orientation purposes some rules of thumb are noted first. The mechanism of initial value growth is similar to that described in the Couette problem except for the reinterpretation of variables previously remarked on. The quantities ψ_x and ψ_z are initially in quadrature so the growth rate is zero at $t = 0$. As the perturbation is sheared by the mean flow it acquires correlations and begins to extract energy from the mean flow. The time scale for this process is $\tau = \ell/k$, the ratio of the vertical to horizontal wavenumbers and the energy extracted increases with vertical wavenumber.

Comparing Figs. 4 and 8, the surprising result is found that for a wavenumber 4 in the vertical initial perturbation and times as large as t=15, corresponding to much of the geophysically relevant interval, the neutral wave at $k = 2.4$ grows as rapidly as the most unstable wave at $k_m = 1.6062$. This behavior persists down to vertical wavenumber 1 although over a somewhat shorter but not insignificant interval in time. It would seem from the observation that neutral waves are able to grow in surface perturbations pressure by nearly three orders of magnitude and by a factor of 100 in shorter time than the most rapidly growing exponential wavenumber, that more emphasis should be placed on the excitation of disturbances than has been the case.

Figures 6 and 7 demonstrate that the exponentially slower growing unstable wavenumber mode at $k = 2.3$ is as efficient out to $t = 15$ in extracting energy from the mean as the most exponentially unstable wavenumber for high vertical wavenumber perturbations.

The neutral waves at $k = 3.0$ (Fig. 10 and 11) extract large amounts of energy from the mean flow for m large and, being equally excited and nonorthogonal, undergo a vacillation cycle (Lindzen et al., in press) with a period given by:

$$T = \frac{2\pi/k}{\Delta c} \tag{28}$$

where:

Δc = difference in normal mode phase speeds.

For $k = 3.0$ the normal modes have phase speeds of $c_1 = .66$ and $c_2 = .33$ resulting in a period from (28):

$$T = \frac{2\pi/3.}{.33} = 6.35 \quad .$$

as may be verified by examining Fig. 10. In Fig. 11, the stream-function snapshots reveal the periodic vacillation in amplitude as the interference progresses. The region of dense samples should be viewed as an approximate envelope as the amplitude changes rapidly between samples.

2.7 The Green Problem

A more realistic model results when the β-effect is included. To this end (20) is restricted to linear shear, $U(z) = z$, the β-plane approximation is made, the Bousinesq approximation is made and rigid horizontal boundaries are imposed at $z = 0,H$. The nondimensional equation is (Lindzen et al., 1980):

$$(z-c)\left(\frac{\partial^2}{\partial z^2} - k^2\right)\psi + r\psi = 0 \tag{29a}$$

$$(z-c)\psi_z - \psi = 0 \qquad z = 0,1 \tag{29b}$$

where the geostrophic streamfunction has been assumed to take the form:

$$\Psi = \psi(z)e^{ik(x-ct)}$$

and

$$r = \frac{\beta H}{\varepsilon \Lambda} \quad \text{stability parameter} .$$

This nondimensional equation has one stability parameter, r which for mid-latitude scaling is:

$$r = \frac{\beta H}{\varepsilon \Lambda} = \frac{(1.6 \times 10^{-11}\ s^{-1} m^{-1})(8 \times 10^{3}\ m)}{(1. \times 10^{-4})(1.25 \times 10^{-3}\ s^{-1})} \approx 1.0 \quad .$$

With the choice $r = 1.0$, the eigenvalues of the discrete normal modes are as shown, Fig. 12a. There are two such modes at each value of k (except

for the isolated point separating the two regions of instability) an exponentially growing mode with the eigenvalue shown and a complex conjugate decaying mode not plotted in Fig. 12a.

Eigenmodes are shown in Fig. 12b for $k_m = 1.8$ near the maximum exponential instability wavenumber and at $k = 6.0$ near the wavenumber at which absolute instability is expected (Farrell, in press), Fig. 12c.

Integrations were performed for k=1.8 and initial perturbations of vertical wavenumber $\ell = m\pi$, $m = 0,2,4,8$ with the results shown, Fig. 13. Stream-function amplitudes are also shown, Fig. 14. In addition results were obtained for $k = 3.0$, Figs. 15 and 16, and for $k = 6.0$, Figs. 17 and 18.

The maximum exponential normal mode growth wavenumber $k_m = 1.8$ benefits marginally from the initial value growth and in fact is weakened out to $t = 10$ for $m = 4$, the correlations being set up slowly for this case (Figs. 13 and 14). The surprising result is the rapid initial growth of the $k = 3.0$ and $k = 6.0$ wave, seen in Figs. 15 through 18, for vertical wavenumber $\ell = m\pi$, $m = 2$ and $m = 4$. The very rapid initial setup of the short wavelength $k = 6.0$ mode and the fact that it is near the absolute instability wavelength (Farrell, in press) suggest a role in cyclogesesis which will be discussed further in the sequel.

2.8 An Equilibrated Flow

Recent work has focused attention on linearly equilibrated zonal flows (Lindzen et al., 1980, Lindzen and Farrell, 1980, Stone, 1978). An example of such an equilibrated stationary solution is the above problem with the zonal velocity $u(z)$ modified so as to render $q_y \geq 0$ everywhere and $u = du/dz = 0$ at $z = 0$, (Lindzen and Farrell, 1980):

$$r - \frac{d^2u}{dz^2} = 0 \qquad 0 \leq z < 1 \tag{30}$$

which has the solution for the above boundary conditions:

$$U(z) = \frac{r}{2} z^2 \tag{31}$$

which for $r = 1.0$ gives the stable to exponentially growing normal mode velocity profile:

$$U(z) = \frac{z^2}{2} \qquad 0 \leq z \leq 1 \quad . \tag{32}$$

Integrations were performed for $k = 3.0$ and initial perturbation vertical wavenumbers $\ell = m\pi$, $m = 0,2,4,8$. The growth rate as a function of time is shown in Fig. 19 with associated streamfunctions, Fig. 20.

At first glance, it may seem that with the potential vorticity of the mean equal to zero throughout the interior and at the lower boundary that a severe restriction on growth of the kind detailed in Appendix 1 for the Couette problem could be imposed. However, there is a source of vorticity in the region of the upper boundary and examination of Fig. 20

shows that the high vertical wavenumber perturbation grows rapidly near this boundary, obtaining two orders of magnitude amplification of perturbation pressure for $m = 4$.

Perturbations to this exponentially stabilized flow extract energy as an initial value problem and obtain maximum perturbation amplitude at the upper level in contrast to the Green normal mode (Fig. 16), which has its maximum at the lower boundary. We note that model studies (Simmons and Hoskins, 1978) have found similar behavior of disturbances in equilibrated mean flows. Although nonlinear effects are important in their work, the parallel is nonetheless suggestive.

The energy extracted from the mean is deposited asymptotically in two neutral waves with phase speeds $c_1 = 0$, and $c_2 = .165$ resulting in a vacillation as discussed previously with period from (28) of:

$$T = \frac{2\pi/3.0}{.165} = 12.7$$

which may be verified by examination of Fig. 19.

It is remarkable that a phase speed zero wave which supports no overreflection (Lindzen et al., 1980) obtains large amplitude in the initial value problem.

2.9 Discussion and Conclusion

Perturbations to stationary solutions of the equations for baroclinic flows are able to extract energy from the mean state whether exponentially growing instabilities are allowed or not. In cases with such exponential modes, the degree to which the mode is excited is dependent on the initial condition so that the initial setup of the instability may proceed much more rapidly than would be predicted for the pure normal mode initial condition.

If cyclogenesis is initiated by a finite amplitude perturbation the structure of the perturbation, in particular its vertical wavenumber, is crucial to the early stages of growth. The total amplification of a disturbance to a geophysical flow may be only a few e-foldings, say in going from a 5 mb depression to a 40 mb surface cyclone, in which case the growth may proceed to nonlinear equilibration without ever obtaining discrete normal mode form. While not of normal mode form, the growing perturbation will of necessity exhibit the phase tilt to the west which marks the extraction of mean flow available potential energy; it is necessary to look closely at the structure of a wave to determine if it has reached normal mode form.

An exact solution of the Eady problem for a zonally localized pulse of vertical wavenumber zero has been obtained (Simmons and Hoskins, 1979) which supports the results obtained in Section 5.

In this example a pulse of uniform amplitude in the vertical and horizontal structure:

$$\nabla_h^2 \psi = A \cos^2 \frac{\pi x}{L} \exp\left(-\frac{x^2}{d^2}\right) \sin \frac{\pi}{y}$$

$y = 5000$ km

$L = 30000$ km

$d = 1000$ km

develops as an initial value problem with

the growth of the perturbation much more rapid than the usual normal mode theory predicts. The attempt to explain this growth by appeal to exponential pulse asymptotics fails as detailed in the reference. In fact, these results give confidence that a major simplification of the analysis of Section 5 does not qualitatively effect the results: the restrictions to infinite meridional scale and a single wavenumber perturbation in x. The geophysically important pulse growth appears to be dominated by small time rather than large time asymptotics.

A baroclinic wave which causes the equilibration to exponential instability of a mean flow does not immediately lose the velocity/temperature correlations which result in the extraction of energy from the mean and will continue to grow. As shown in section 9, the eigenfunctions which are excited in initial value integrations for an equilibrated flow have maximum amplitude and take energy from the mean at high levels in the model atmosphere, corresponding to the region where $\pi_y > 0$. This contrasts with the eigenfunctions before equilibration which have maximum amplitude and extract energy at low levels.

If such equilibration of mean flows is a common occurrence as has been recently argued (Lindzen and Farrell, 1980) then the secondary maxima of heat flux and wave amplitude in the upper troposphere seen both in observations and model experiments (Simmons and Hoskins, 1978) is to be expected.

If zero vertical wavenumber is effective in promoting growth of perturbations then, as has been shown above, higher wavenumbers are even more effective. It is appropriate to ask if such complex vertical structure is found in the atmosphere. Note first that the vertical derivative of potential vorticity corresponds to a temperature perturbation.

It is unfortunate that observed temperature profiles are usually extensively smoothed obscuring the information on vertical structure; however, even in the smoothed data there is found evidence of large scale coherent high wavenumber structure (Buzzi and Tibaldi, 1978; their Figs. 5 and 8; Hess and Wagner, 1948, their Figs. 7 and 8). Whether this structure serves as an initial condition in its own right or induces structure on a quasi-barotropic perturbation would be a subject for another investigation.

It may be appropriate to indulge a speculation on rapid cyclogenesis. The energy growth curves discussed in Section 8 for high wavenumber vertical perturbations bear a striking resemblance to growth curves for Alpine cyclogenesis (Buzzi and Tibaldi, 1978; their Fig. 12) and data for the initial stages of rapid cyclogenesis (Sanders and Gyakum, 1980). Attempts to relate these growths to exponential normal mode analysis fails in both these references as it did in Simmons and Hoskins (1978). The horizontal scale of the waves is small at first and increases as they consolidate into normal mode form late in the development, in agreement with pulse asymptotic theory (Farrell, in press). Concentrating on the rapid first stage of growth, the fact that a sudden change in the wind velocity, whether from a trailing cold front (Buzzi and Tibaldi, 1978; their Fig. 1) or an advancing trough (Sanders and Gyakum, 1980 . Hess and Wagner 1948), is the immediate precursor of the cyclogenesis suggests that a stationary wave which was in equilibrium with the flow before the front passed has been "cut loose" by the rapid change of velocity to serve as the initial condition for the cyclogenesis. This mechanism agrees with the coincidence of regions of explosive cyclogenesis and mountains if

we are willing to consider the Atlantic and Pacific Western boundary currents as "thermal mountains." The waves would have to be of large horizontal extent $\lambda > 600$ km which rules out pure gravity waves but agrees with observations of combined inertia-gravity waves (Hess and Wagner, 1948 , Sawyer, 1960). The manner in which these waves would in the course of collapsing serve as initial perturbations for quasi-geostrophic baroclinic waves is subject for a model study.

Finally, we remark that if the growth of cyclone waves is dependent on the vertical structure of the initial condition to the extent found here, stringent requirements are implied for vertical resolution both in observations and numerical simulations.

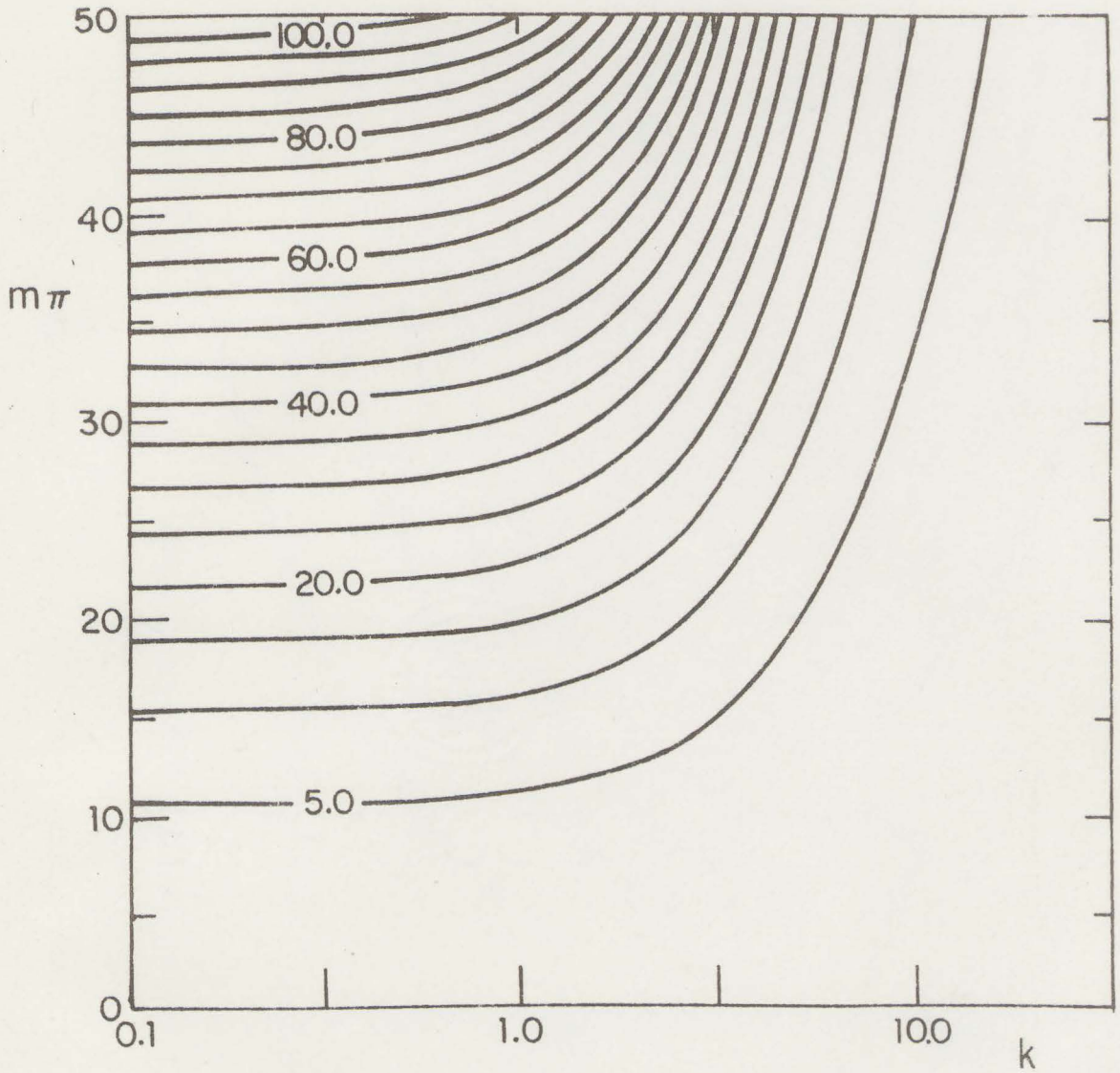

Fig. 1a Approximate maximum normalized kinetic energy for the Couette problem as a function of perturbation horizontal wavenumber, k and vertical wavenumber $m\pi$.

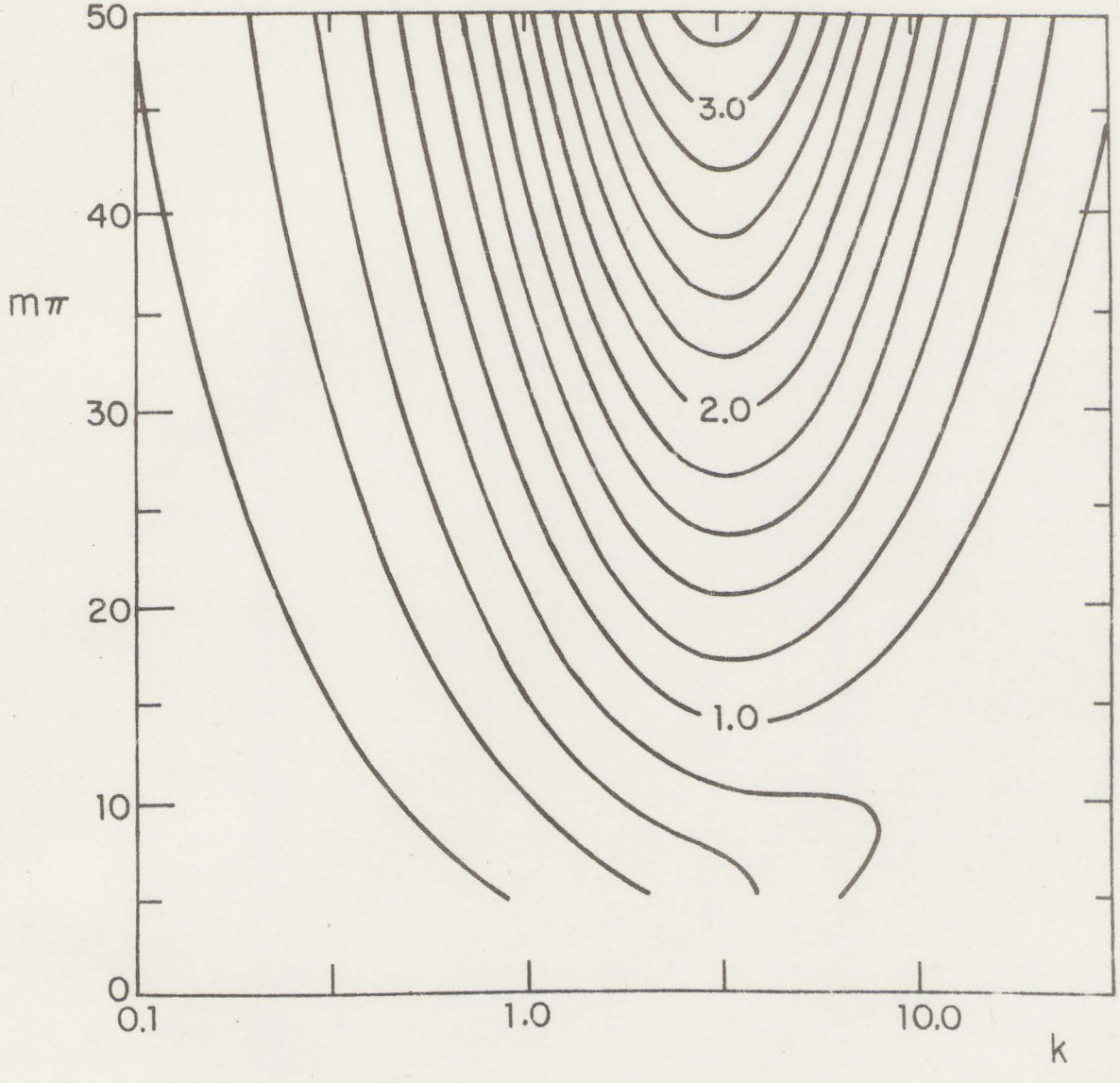

Fig. 1b Approximate growth rate of perturbations for the Couette problem as a function of perturbation horizontal wavenumber, k and vertical wavenumber mπ.

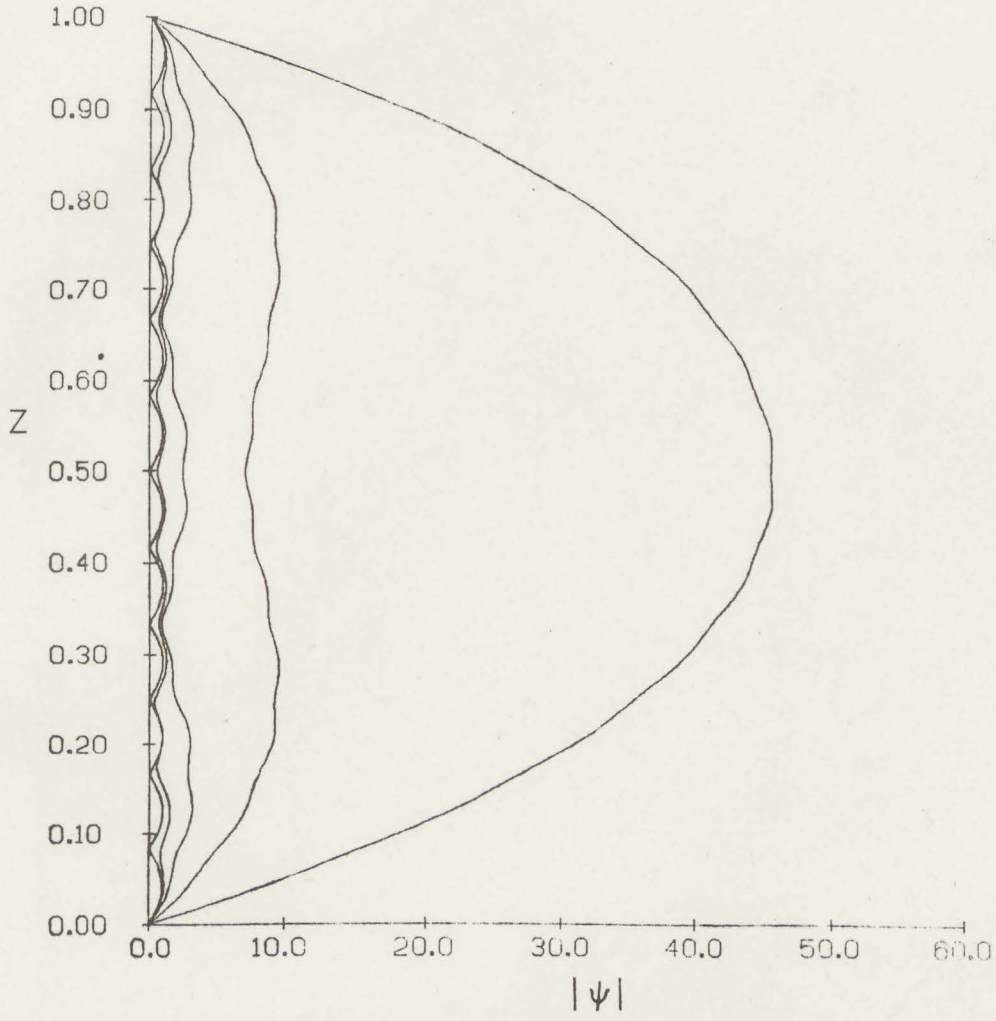

Fig. 2a Magnitude of the streamfunction for the Couette problem as a function of time for perturbation horizontal wavenumber k = 3.0, and vertical wavenumber, $\ell = 12\pi$. Time is scaled by nn/k: $\tilde{t} = t/(nn/k)$. Streamfunctions for $\tilde{t} \leq 1.0$ are shown.

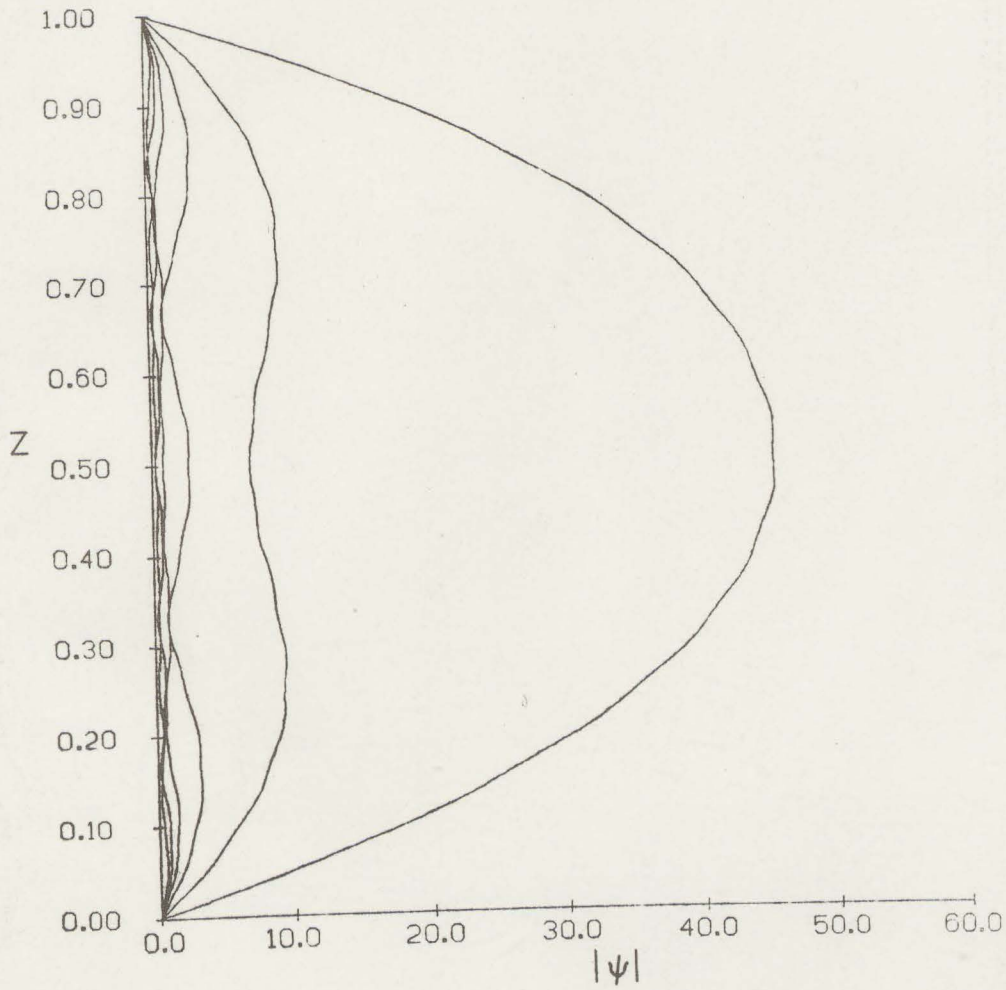

Fig. 2b Same as 2a except for $\tilde{t} \geq 1.0$.

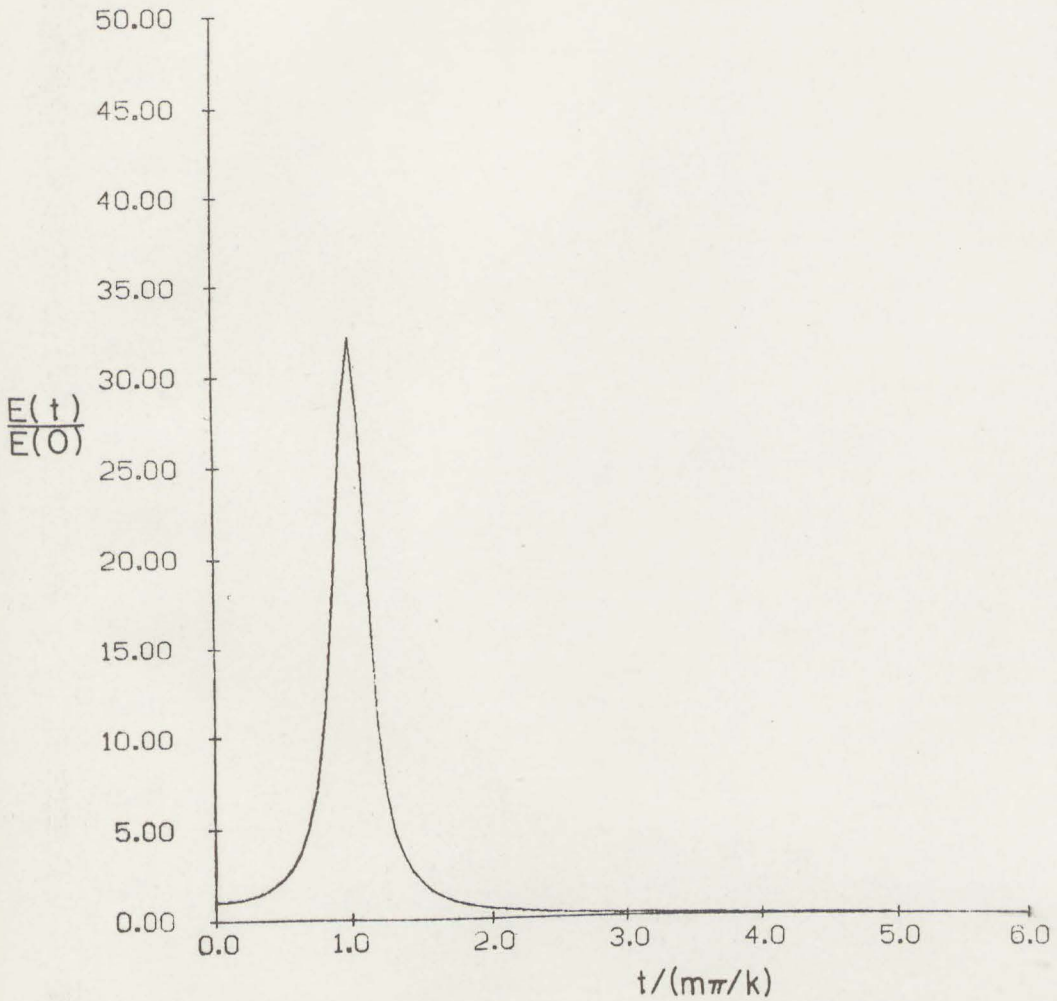

Fig. 2c Exact normalized energy as a function of time for the example in Fig. 2a.

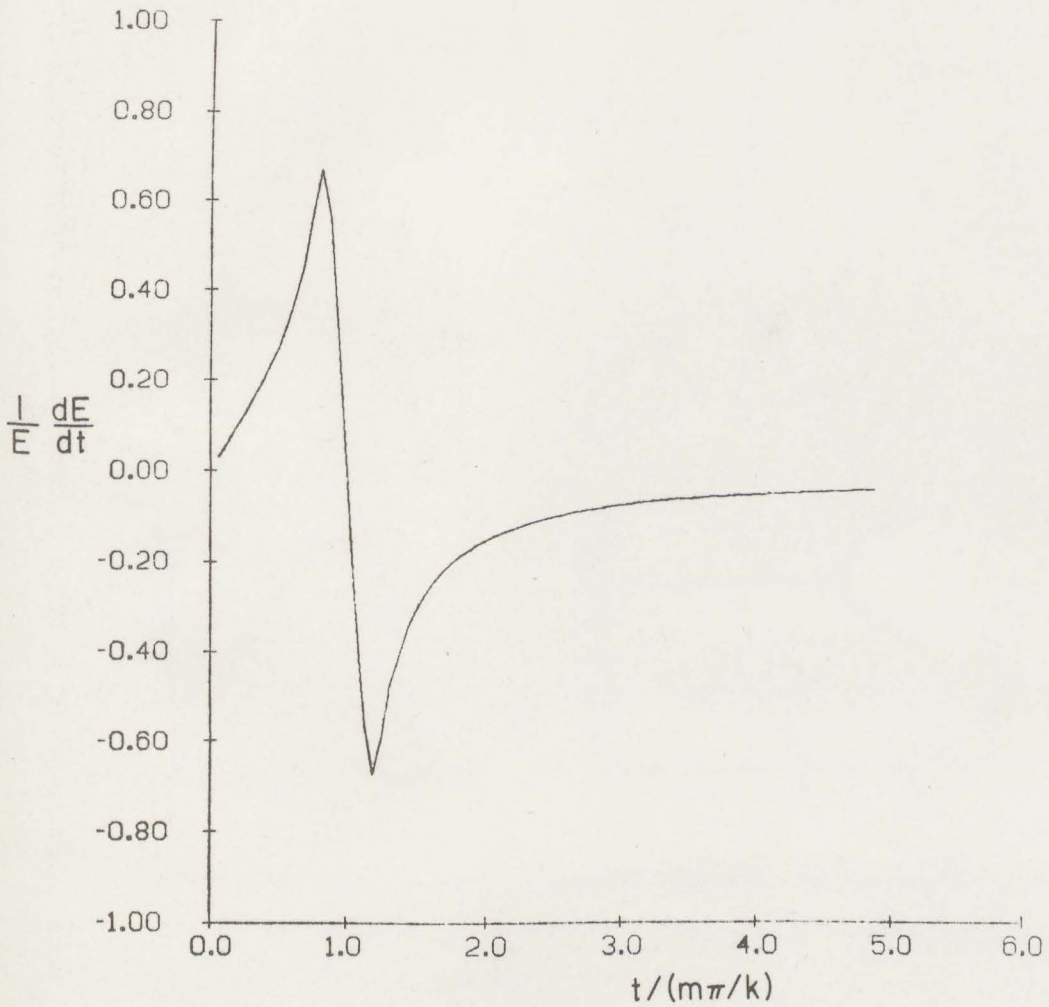

Fig. 2d Energy growth rate $2kc_{i_{eff}} = 1/E\ dE/dt$ as a function of scaled time $\bar{t} = t/(m\pi/k)$, for the example in Fig. 2a.

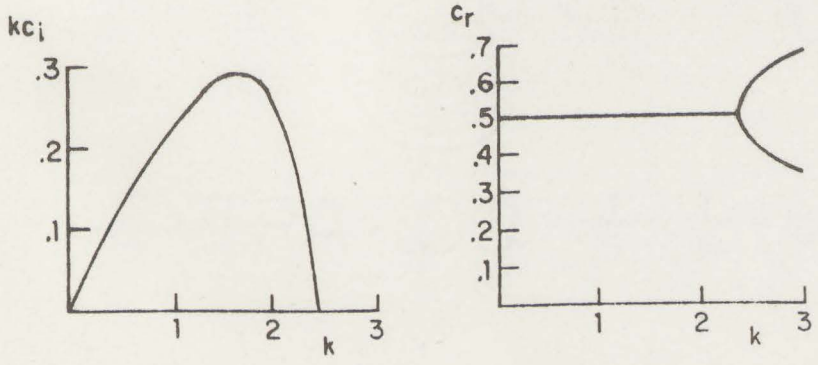

Fig. 3a Phase speed, c_R and growth rate, kc_i for the discrete normal modes in the Eady problem. There is also a complex conjugate decaying mode for $0 < k < 2.3994$.

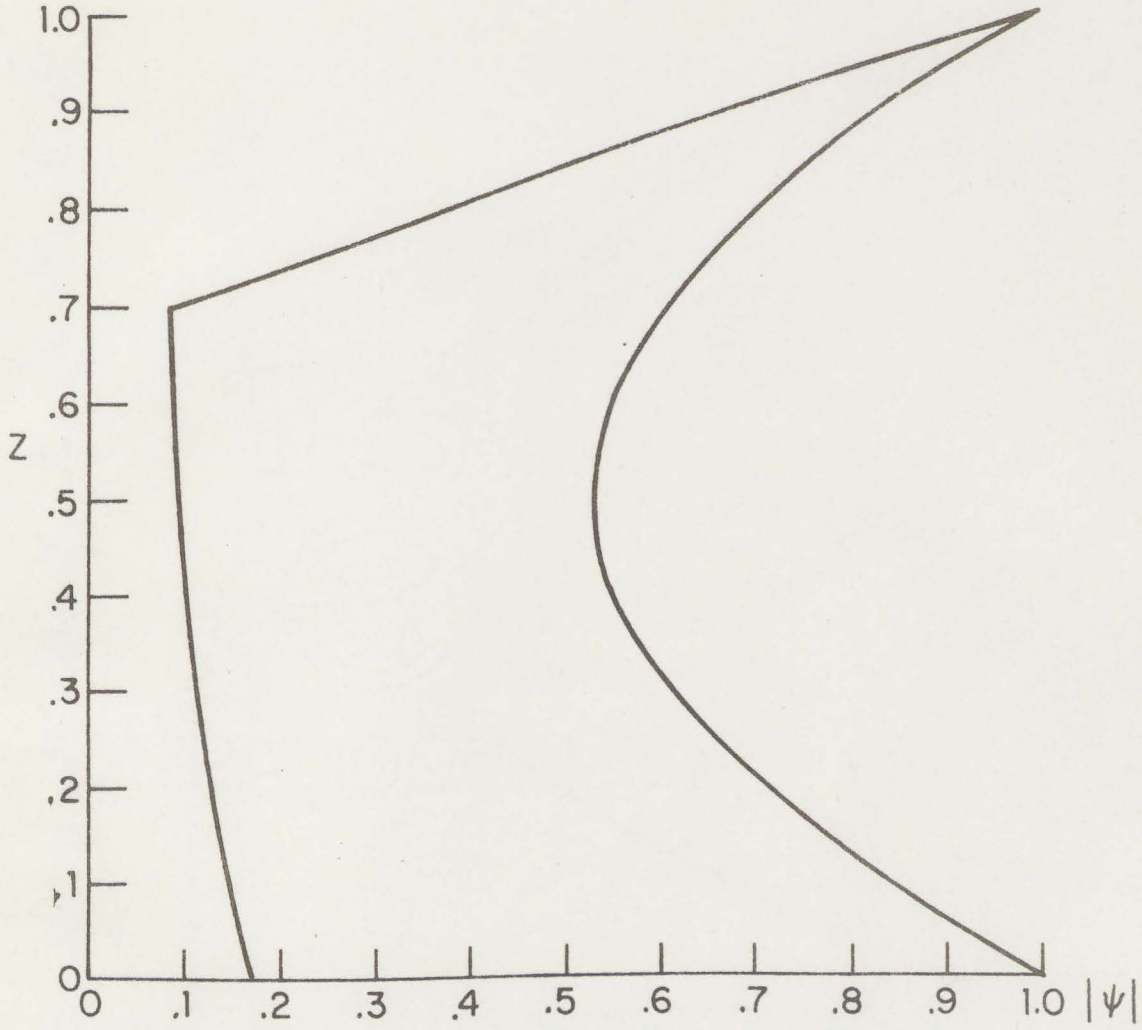

Fig. 3b Normal mode streamfunction amplitude at horizontal wavenumber $k_m = 1.6062$ for the Eady problem. An example of the continuum normal modes at $c = .7$ is shown.

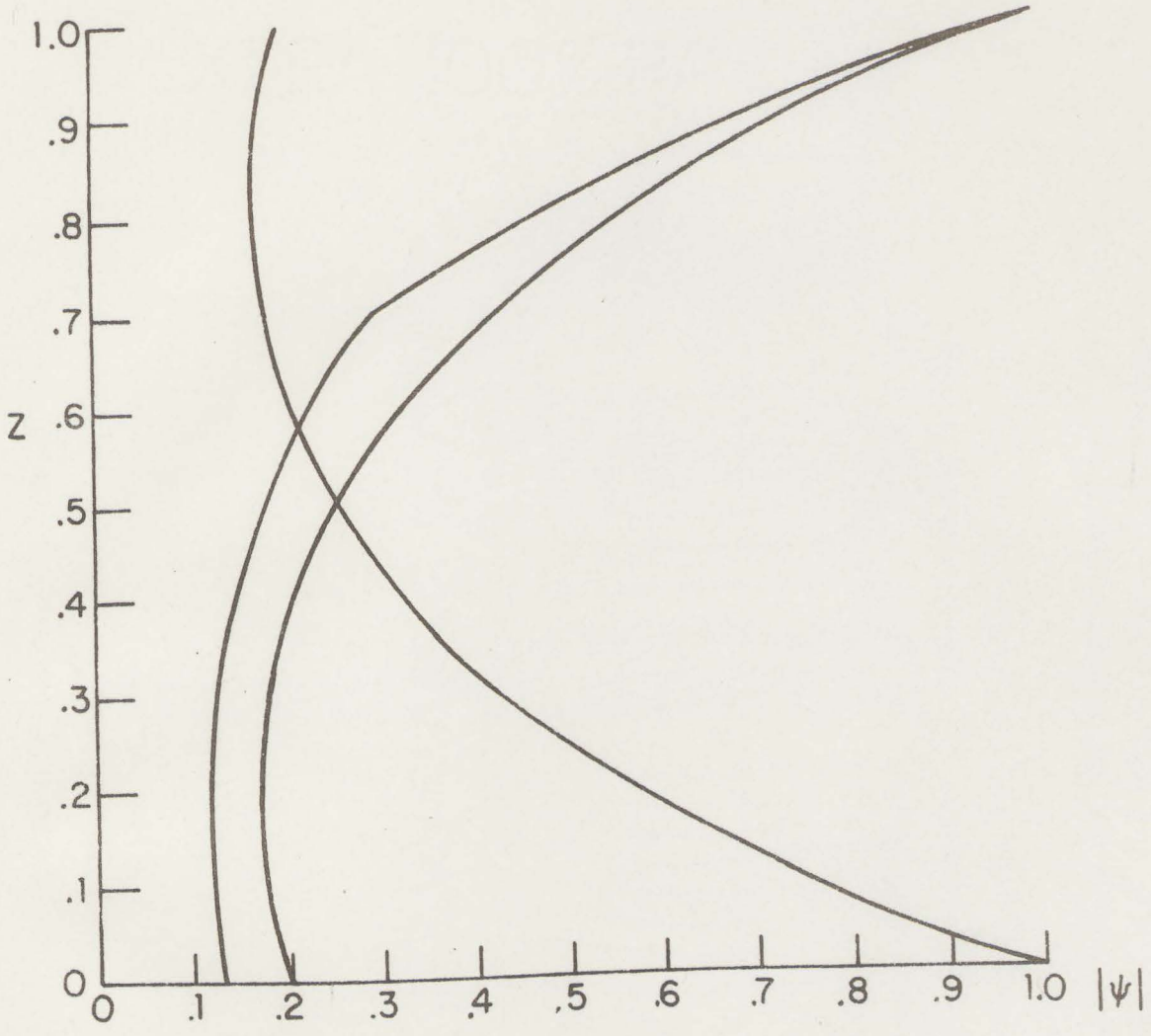

Fig. 3c Same as 3b except for $k = 3.0$ in the neutral region.

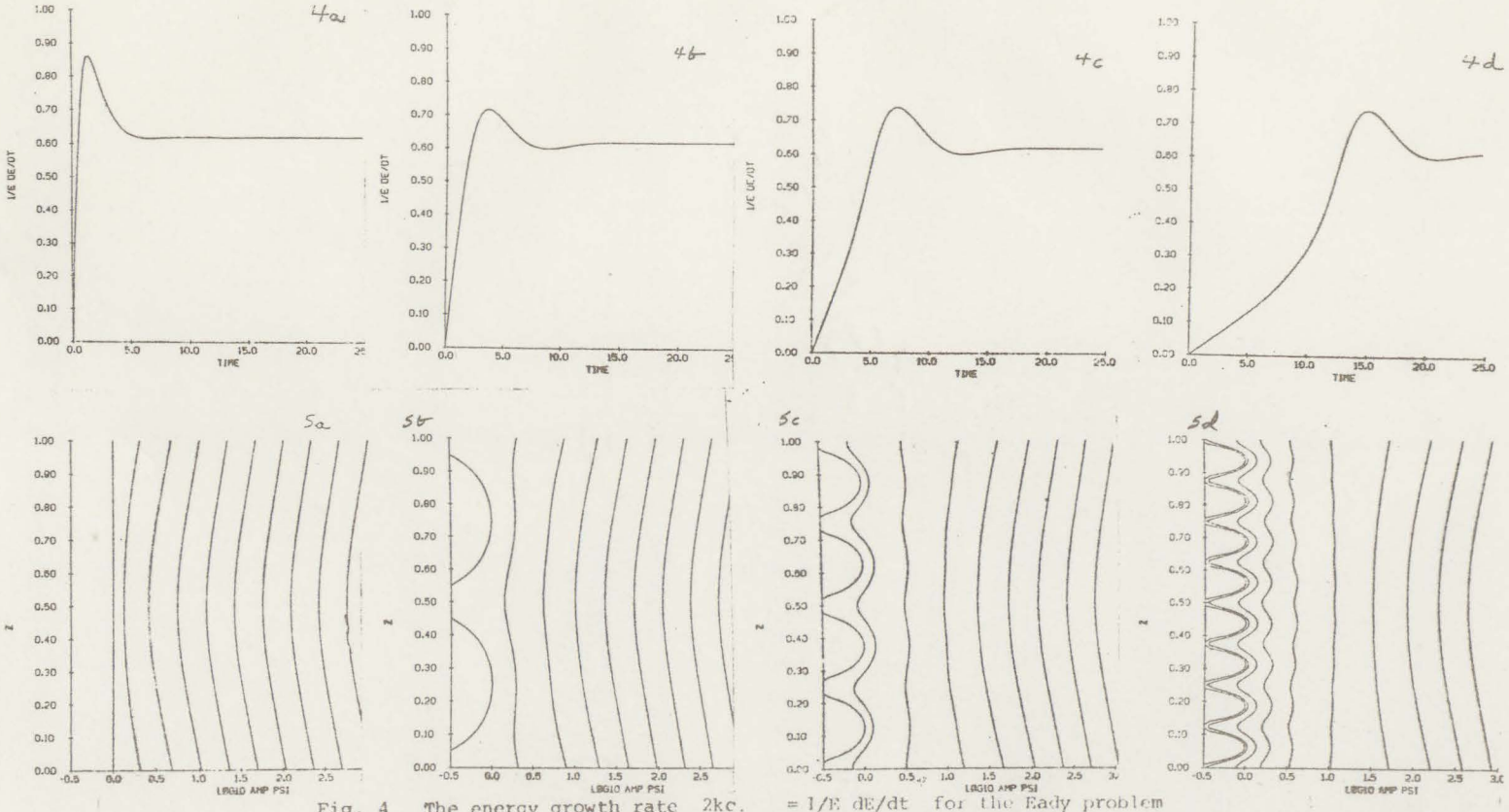

Fig. 4 The energy growth rate $2kc_{i_{eff}} = 1/E\ dE/dt$ for the Eady problem with horizontal wavenumber $k_m = 1.6062$ and initial perturbation vertical wavenumber $\ell = m\pi$, $m = 0,2,4,8$; Fig. 4a, 4b, 4c, 4d respectively.

Fig. 5 Streamfunction amplitude for the examples in Fig. 4 as a function of height, z. Samples are taken at $T = N\Delta T$, $N = 0,1,2 \ldots 9$; Fig. 5a, 5b, 5c, 5d respectively.

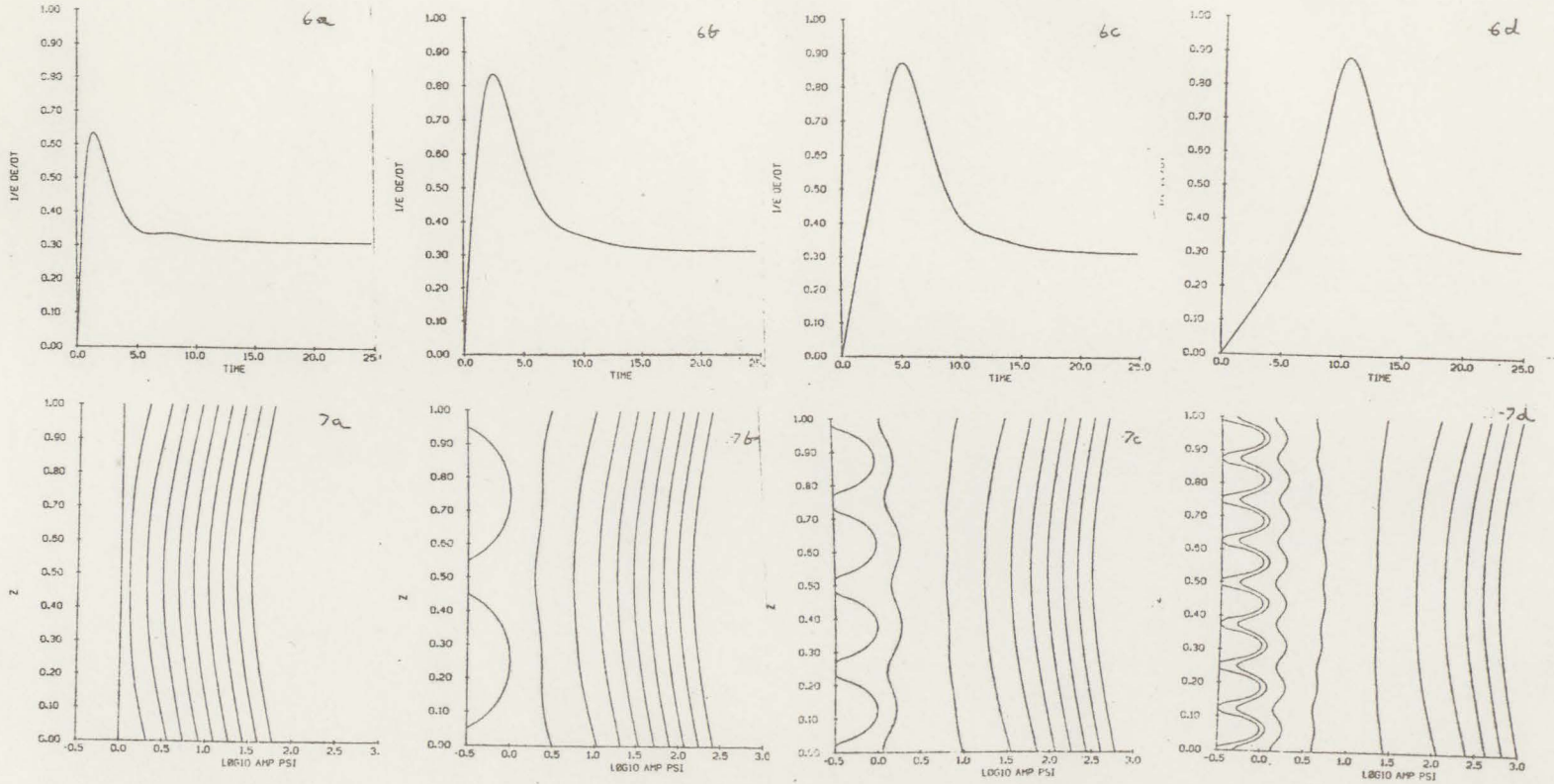

Fig. 6 Same as Figure 4 except k = 2.3.

Fig. 7 Same as Figure 5 except k = 2.3.

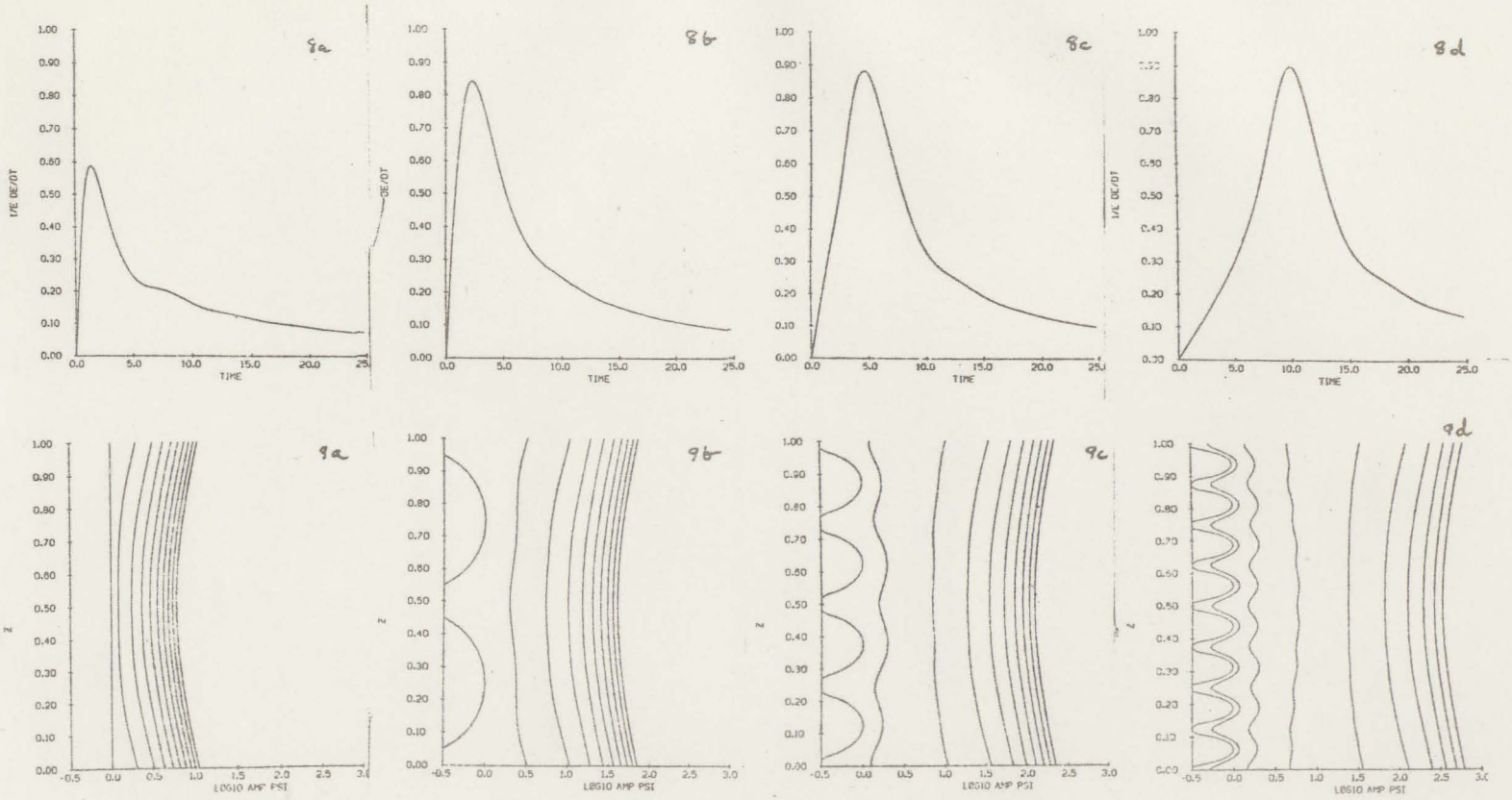

Fig. 8 Same as Figure 4 except k = 2.4.

Fig. 9 Same as Figure 5 except k = 2.4.

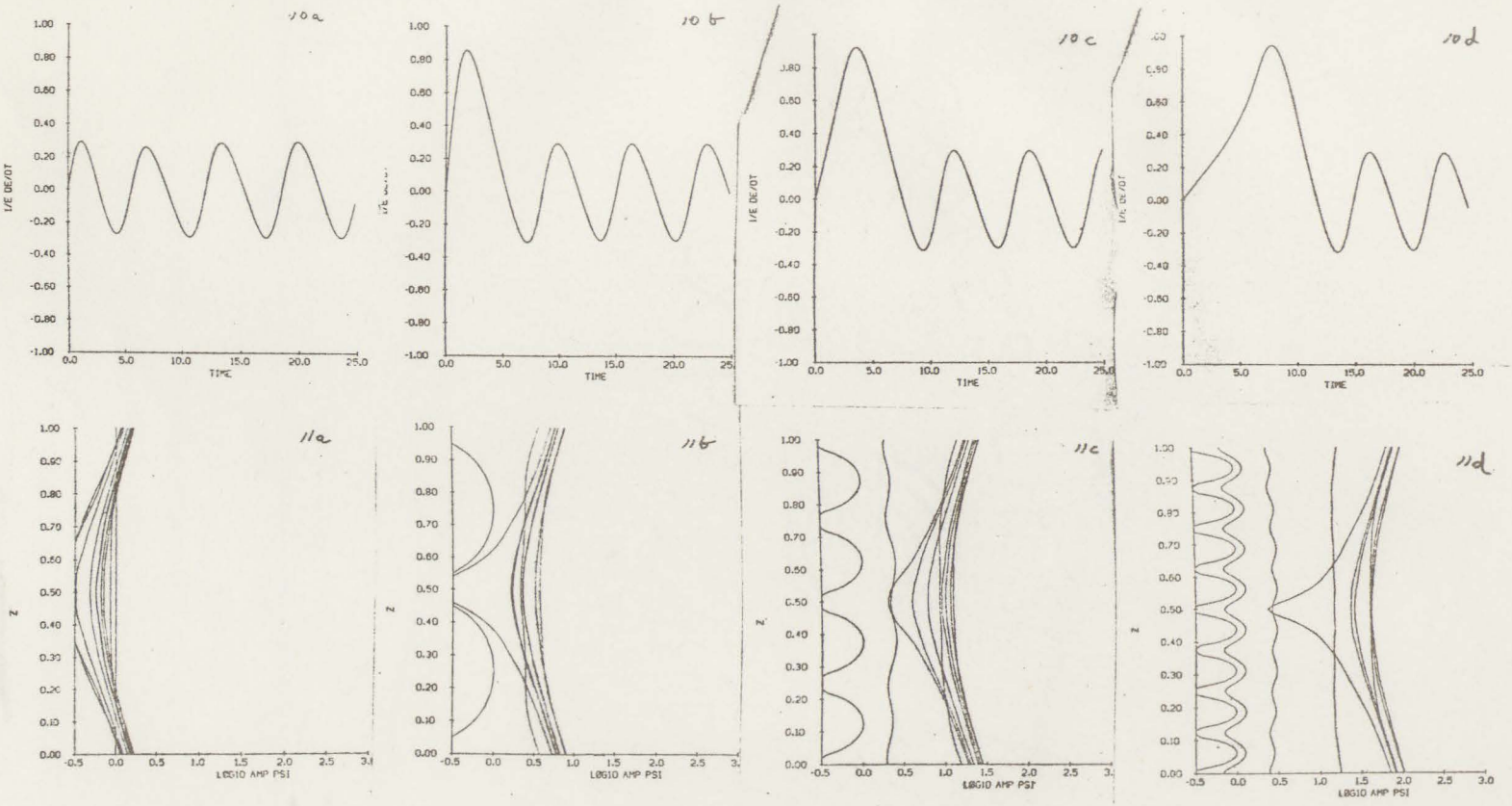

Fig. 10 Same as Figure 4 except k = 3.0.

Fig. 11 Same as Figure 5 except k = 3.0.

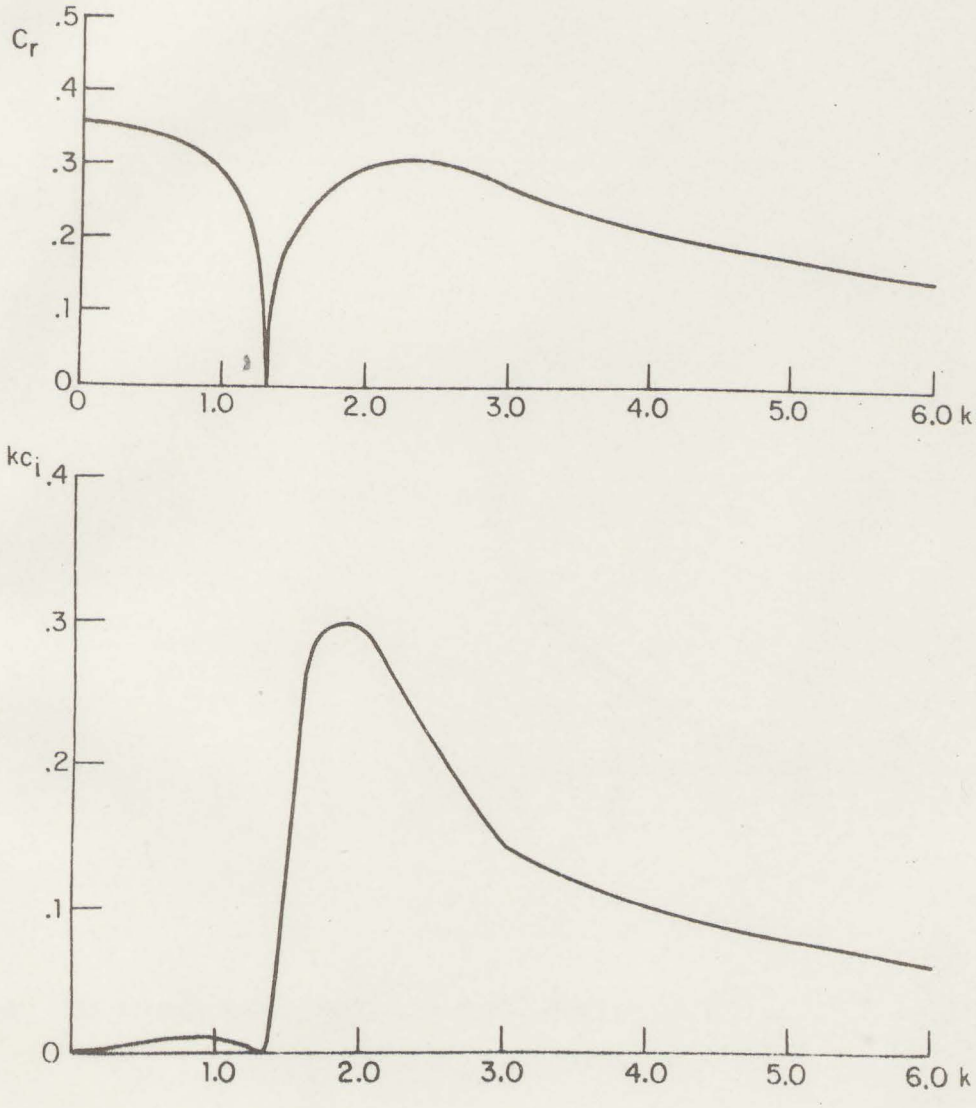

Fig. 12a Phase speed, c_r and growth rate, kc_i for the discrete normal modes in the Green problem. There are also complex conjugate decaying modes.

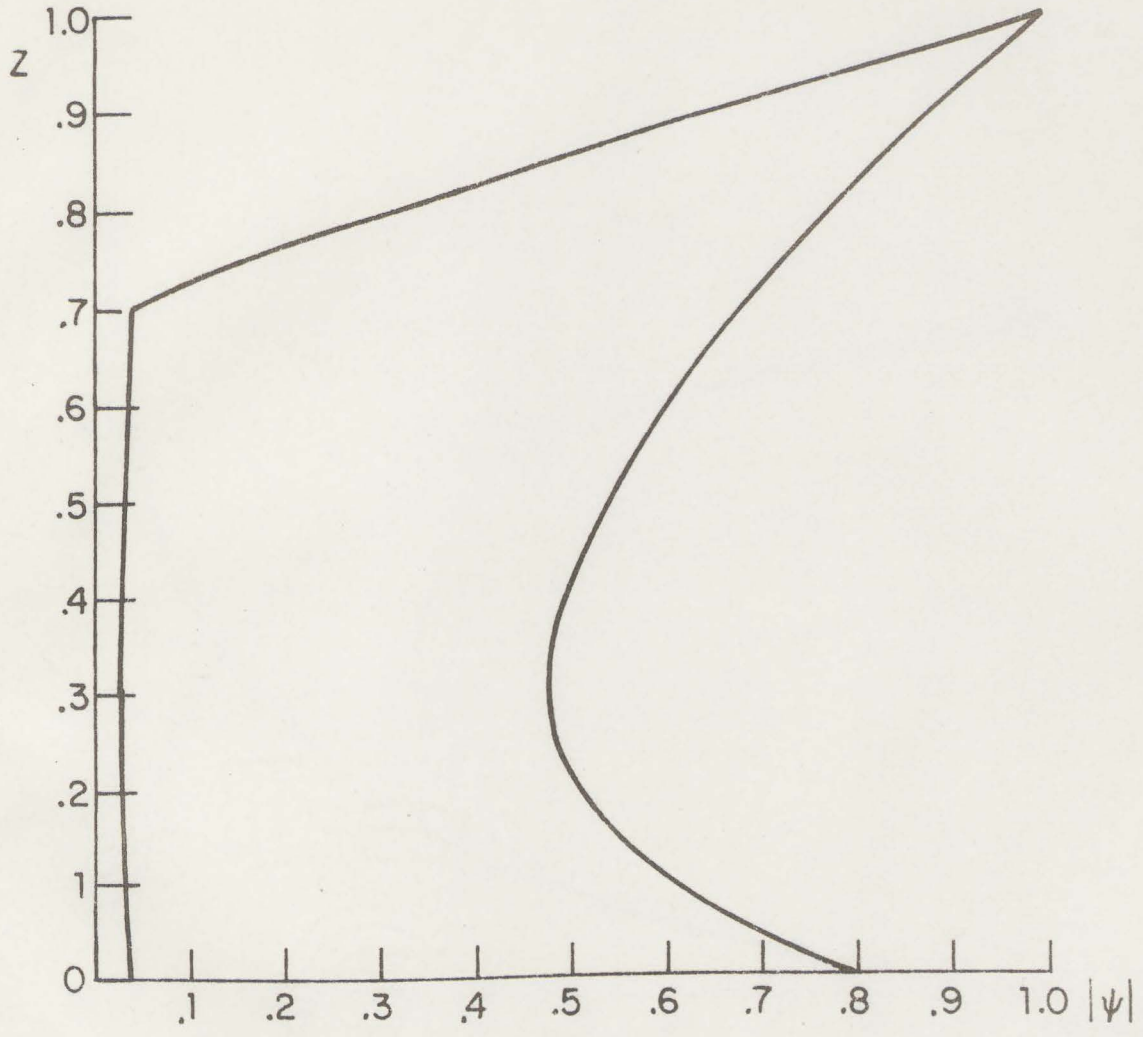

Fig. 12b Normal mode streamfunction amplitude at $k_m = 1.8$, together with the continuum normal mode at $c = .7$.

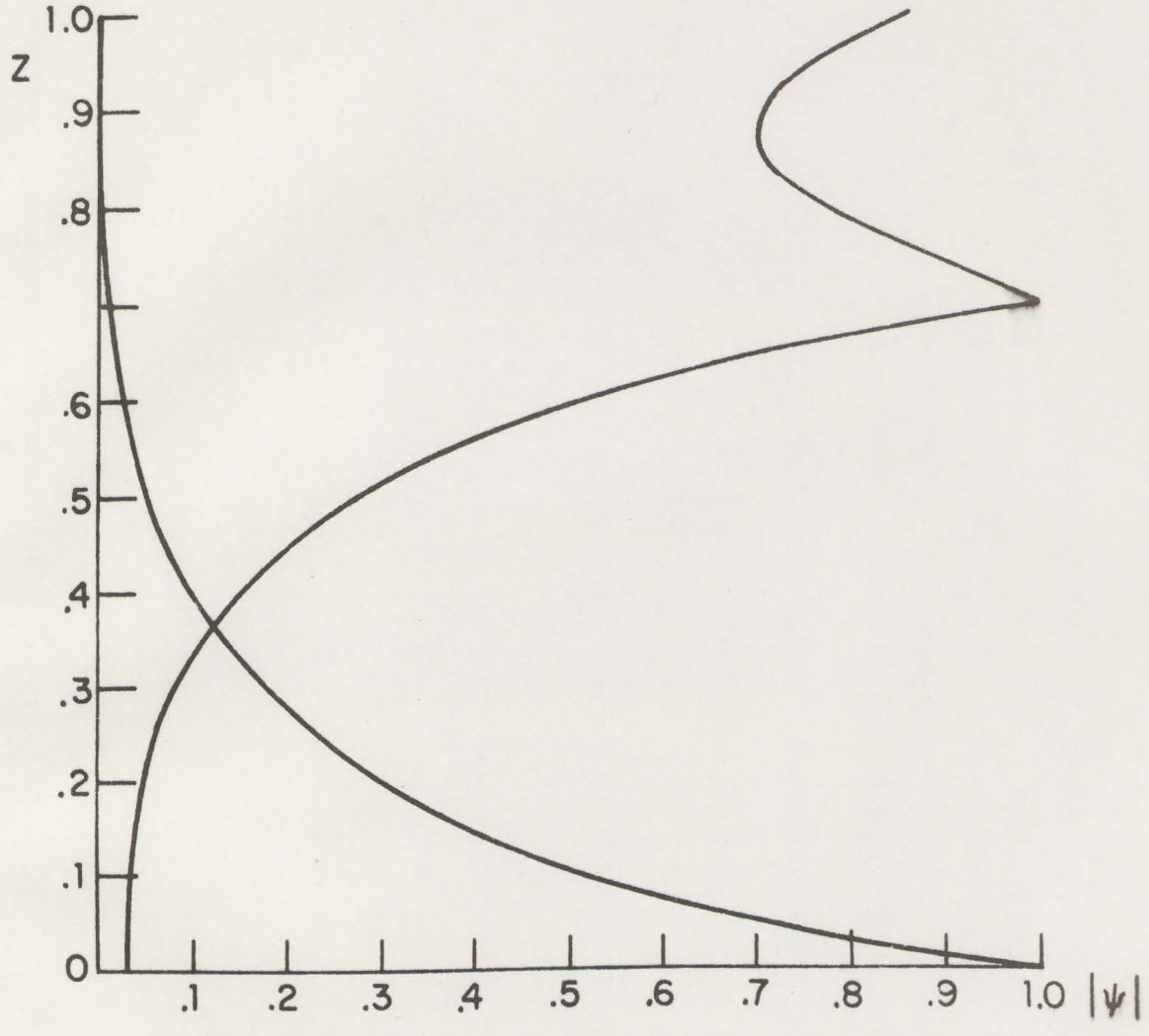

Fig. 12c Same as Fig 12b except for k = 6.0.

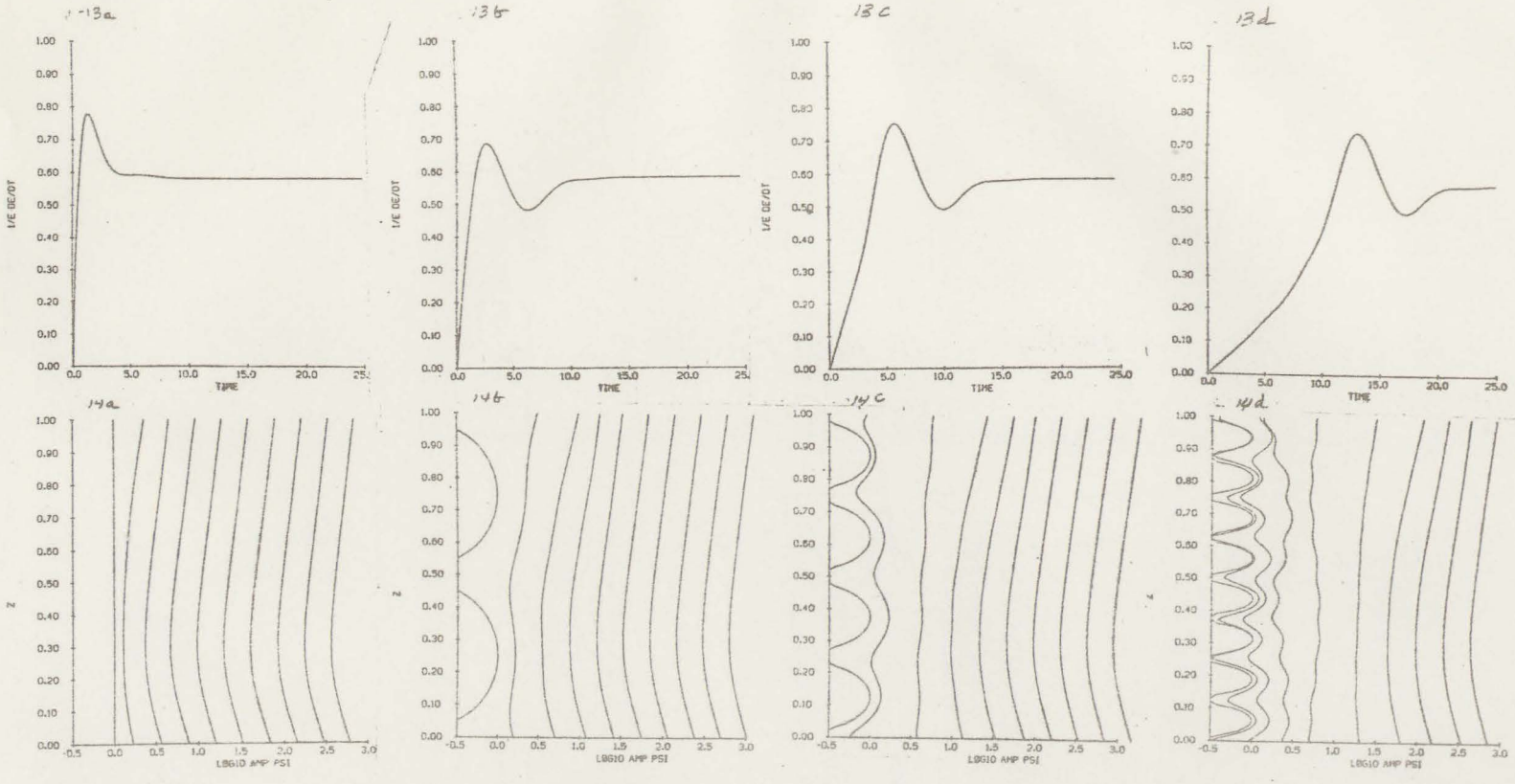

Fig. 13 The energy growth rate $2kc_{i_{eff}} = 1/E\ dE/dt$ for the case in Fig. 12 with horizontal wavenumber $k_m = 1.8$ and perturbation vertical wavenumber $\ell = m\pi$, $m = 0,2,4,8$; Fig. 13a, 13b, 13c, 13d respectively.

Fig. 14 Streamfunction amplitudes for the examples in Fig. 13.

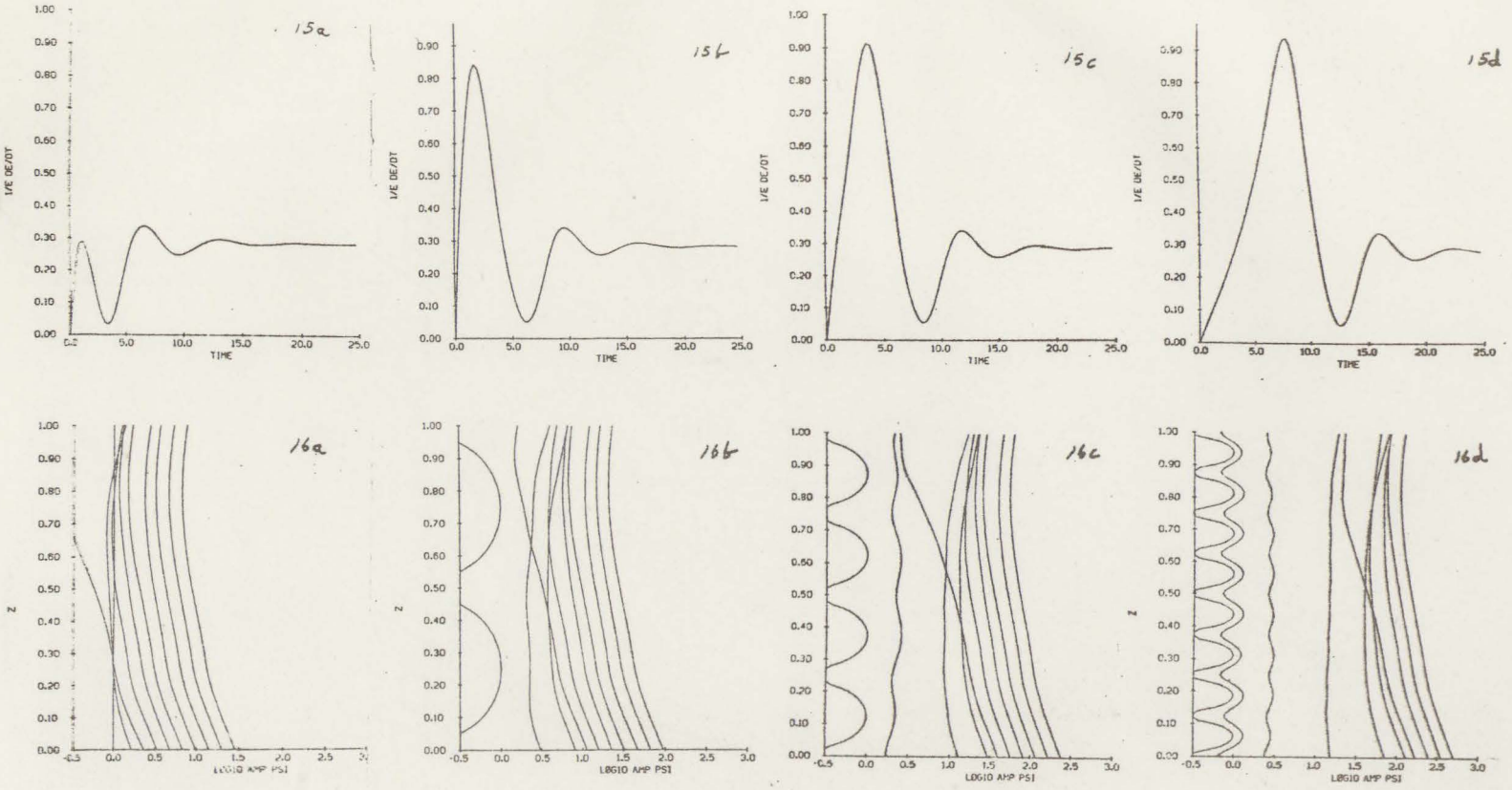

Fig. 15 Same as Fig. 13 except k = 3.0.

Fig. 16 Same as Fig. 14 except k = 3.0.

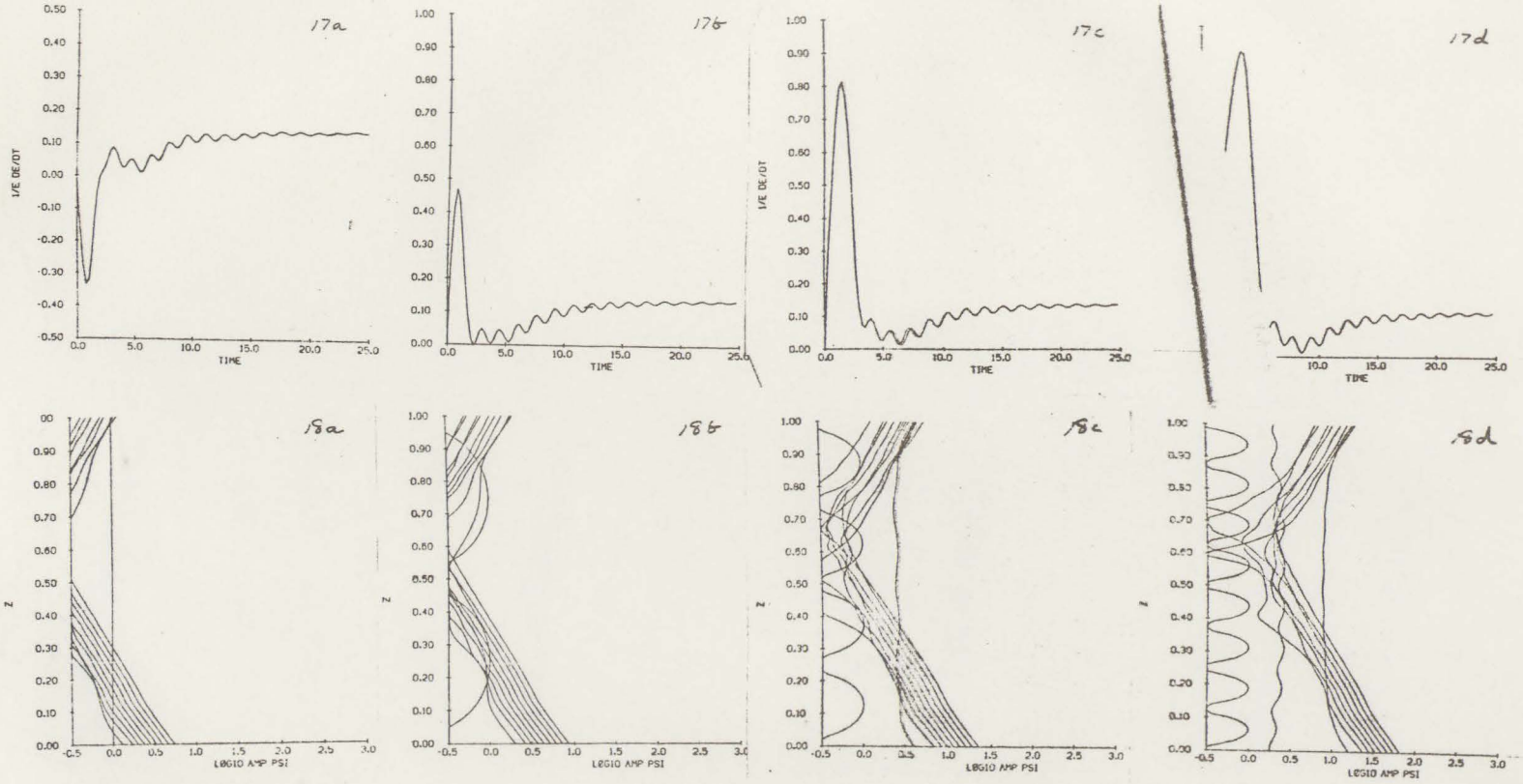

Fig. 17 Same as Fig. 13 except for $k = 6.0$.

Fig. 18 Same as Fig. 14 except for $k = 6.0$.

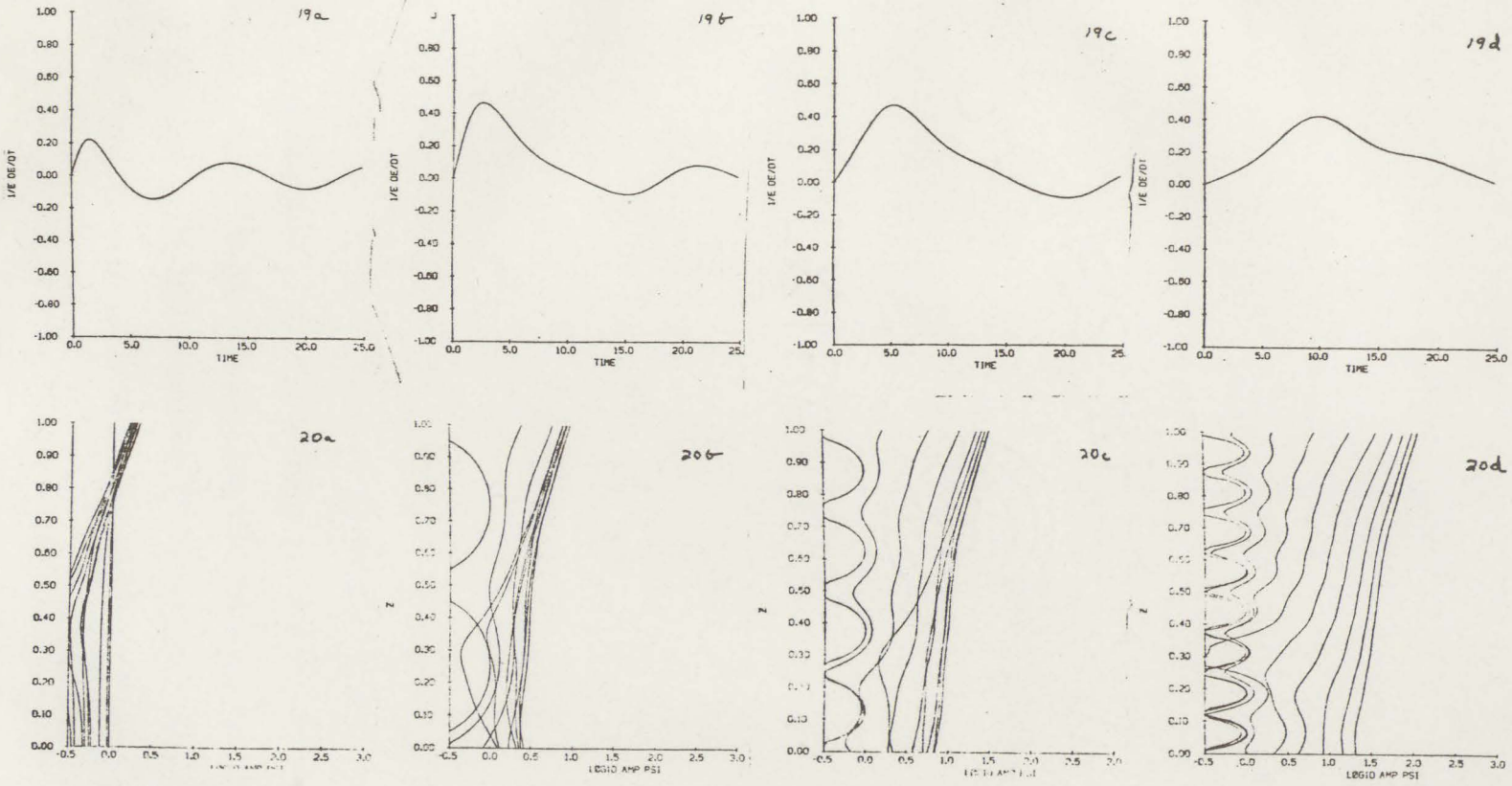

Fig. 19 Same as Fig. 15 except for equilibrated profile

Fig. 20 Same as Fig. 16 except for equilibrated profile

APPENDIX D

The basic state for the Couette problem possesses no vorticity, and in inviscid dynamics there is no other source of vorticity except the initial perturbation. This fact may be exploited to obtain a bound on the initial value growth.

Consider an initial perturbation of horizontal wavenumber k and vertical wavenumber $m\pi$:

$$\psi = A_i \sin m\pi z \cos kx$$

The energy from (15) is:

$$E = \frac{A_i^2((m\pi)^2 + k^2)}{4} \quad . \tag{A1}$$

The enstrophy is given by:

$$\xi = \int_0^1 \frac{1}{2} (\bar{\psi}_{xx} + \bar{\psi}_{zz})^2 \, dz$$

$$= \frac{A_i^2((m\pi)^4 + k^4)}{4} \quad . \tag{A2}$$

As ξ is a constant for the flow, it must also be the enstrophy of the mode which maximizes E. The problem of maximizing E subject to the constraint that ξ be constant and the boundary conditions (1b) are met may be solved using the formalism of the variational calculus. For our purposes it will suffice to note that maximum energy is associated

with minimum vertical wavenumber and choose the approximate maximum energy state as $m = 1$:

$$\psi_m = A_m \sin \pi z \cos kx \quad .$$

If the initial perturbation has wavenumber $m\pi$ then the constancy of ξ requires from (A2):

$$\frac{A_m^2}{4} (\pi^4 + k^4) = \frac{A_i^2}{4} ((m\pi)^4 + k^4) .$$

Hence the initial and approximate maximum amplitudes are related by:

$$A_m^2 = A_i^2 \frac{(m\pi)^4 + k^4}{\pi^4 + k^4} \quad .$$

The approximate maximum energy from (A1) is:

$$E_m = A_i^2 \frac{(m\pi)^4 + k^4}{\pi^4 + k^4} \frac{\pi^2 + k^2}{4} \quad .$$

The ratio of maximum to initial energy is:

$$\frac{E_m}{E_i} = \frac{\dfrac{(m\pi)^4 + k^4}{\pi^4 + k^4} \dfrac{\pi^2 + k^2}{4}}{\dfrac{(m\pi)^2 + k^2}{4}} = \frac{(m\pi)^4 + k^4}{(m\pi)^2 + k^2} \frac{\pi^2 + k^2}{\pi^4 + k^4} \qquad \text{(A3)}$$

The limit $k \to 0$ is:

$$\frac{E_m}{E_i} = m^2 \quad . \tag{A4}$$

Whereas for $k = \pi$ near the maximum of growth rate we have:

$$\frac{E_m}{E_i} = \frac{m^4 + 1}{m^2 + 1} \tag{A5}$$

which for $m >> 1$ reduces to (A4). Comparing with Fig. 1 a parallel behavior is seen and the perturbations fail to achieve these approximate maxima by only a small factor. For example as $k \to 0$, (14) reduces to:

$$\lim_{k \to 0} \frac{E_m}{E_i} = \frac{(m\pi)^2}{24} \simeq .41\ m^2 \quad .$$

The above argument may be extended to the decay phase of the initial value problem for which conservation of enstrophy implies that the vertical wavenumber will increase linearly with time to give a t^{-2} decay in amplitude. Figure 2b clearly shows this linear increase in wavenumber. Of course it would be possible for a perturbation to decrease in amplitude by apportioning energy over many wavenumbers so that this argument must be generalized to a Fourier sum (Charney, 1973).

APPENDIX B

With the substitution of (23), the linearized equation for the conservation of potential vorticity (20) can be written:

$$\left(\frac{\partial}{\partial t} + Uik\right)\left(- k^2 + \frac{\partial^2}{\partial z^2}\right)\psi(z,t) - q_y ik\psi(z,t) = 0 \qquad \text{(A1a)}$$

$$\left(\frac{\partial}{\partial t} + Uik\right)\frac{\partial\psi(z,t)}{\partial z} - \frac{dU}{\partial z} ik\psi(z,t) = 0 \qquad z = 0,1 \ . \qquad \text{(A1b)}$$

Forming the matrix operator $\underline{\nabla}^2 = (-k^2 + \partial^2/\partial z^2)$ on $N+2$ points by the usual finite difference approximation to derivatives and using (A1b) to eliminate the outlying boundary points allows (A1) to be written:

$$\frac{\partial}{\partial t}\underline{\nabla}^2\underline{\psi} = -ik[\underline{U}\underline{\nabla}^2 - \underline{q}_y]\underline{\psi} = 0$$

$$\frac{\partial}{\partial t}\underline{\psi} = -ik[\underline{\nabla}^{2^{-1}}\underline{U}\underline{\nabla}^2 - \underline{\nabla}^{2^{-1}}\underline{q}_y]\psi \ .$$

Identifying $\underline{A} \equiv -ik[\underline{\nabla}^{2^{-1}}\underline{U}\underline{\nabla}^2 - \underline{\nabla}^{2^{-1}}\underline{q}_y]$ results in a matrix eigenvalue problem for $\underline{\psi}(z,t)$:

$$\frac{\partial}{\partial t}\underline{\psi} = \underline{A}\underline{\psi} \ . \qquad \text{(A2)}$$

If $\underline{A}$ has N distinct eigenvalues, λ_N then it has N associated linearly independent eigenvectors $\underline{\psi}_N$. As the matrix $\underline{A}$ is not symmetric these $\underline{\psi}_N$ are not in general orthogonal. The solution to (A2) for initial

perturbation $\underline{\psi}(z,0)$ is:

$$\underline{\psi}(z,t) = \underline{\Lambda}\underline{E}\underline{\Lambda}^{-1}\underline{\psi}(z,0)$$

where

$\underline{\Lambda} = [\psi_1 \quad \psi_2 \quad \cdots \quad \psi_N]$ the matrix of eigenvectors

$$\underline{E} = \begin{bmatrix} e^{\lambda_1 t} & & 0 \\ & \ddots & \\ 0 & & e^{\lambda_N t} \end{bmatrix}$$ the matrix of eigenvalue exponentials

The solution as a function of time is, from (23):

$$\underline{\Psi}(x,z,t) = \underline{\psi}(z,t)e^{ikx} \quad .$$

With $\underline{\nabla}^2$ discretized using fourth order differencing on $N = 100$ points the QR algorithm requires less than 10 min to extract the eigenvectors using the modest DEC VAX 11/780 computer.

References

Arnol'd, V.I., 1965. Conditions for nonlinear stability of stationary plane curvilinear flows of an ideal fluid. Doklady, 162, 773-777.

Blumen, W., 1968. On the stability of quasi-geostrophic flow. J. Atmos. Sci., 25, 929-931.

Bretherton, F.P., 1966. Critical layer instability in baroclinic flows. Quart. J. Ray. Meteor. Soc., 92, 325-334.

Brown, S.N., and Stewartson, K., 1980. On the algebraic decay of disturbances in a stratified shear flow. J. Fluid Mech. 100, 811-816.

Burger, A.P., 1966. Instability associated with the continuous spectrum in a baroclinic flow. J. Atmos. Sci., 23, 272-277.

Buzzi, A., and Tibaldi, S., 1978. Cyclogenesis in the lee of the Alps: a case study. Quart. J. Roy. Metero. Soc., 104, 271-287.

Case, K.M., 1960. Stability of inviscid plane Couette flow. Phys. Fluids, 3, 14.

Case, K.M., 1961. Hydrodynamic stability and the inviscid limit. J. Fluid Mech. 10, 420.

Charney, J.G., 1947. The dynamics of long waves in a baroclinic westerly current. J. Meteor. 4, 135-162.

Charney, J.G., 1973. Planetary fluid dynamics. Chapter 2 in Dynamic Meteorology, P. Morel, Editor. D. Reidel Publishing Co., Dordrecht, Holland. pp. 234-236.

Courant, R., and Hilbert, D., 1953. Methods of Mathematical Phsyics. Vol. 1, John Wiley and Sons, New York, pp. 354-358.

Eady, E.J., 1949. Long waves and cyclone waves. Tellus, 1, 33-52.

Farrell, B.F., 1981. Pulse asymptotics of the Charney problem. Submitted to J. Atmos. Sci.

Hess, S.L., and Wagner, H., 1948. Atmospheric waves in the northwestern United States. J. Meteor., 5, 1-19.

Jeffreys, H., and Jeffreys, B., 1956. Methods of mathematical physics. Cambridge University Press, Cambridge, pp. 7/8.

Landahl, M.T., 1975. Wave breakdown and turbulence. SIAM J. Appl. Math., 28, 735-756.

Lin, C.C., 1961. Some mathematical problems in the thoery of the stability of parallel flows. J. Fluid Mech. 10, 430-438.

Lindzen, R.S., B. Farrell, 1980. The role of polar regions in global climate, and a new parameterization of global heat transport. Mon. Wea. Rev. 108, 2064-2079.

Lindzen, R.S., B. Farrell and K.-K. Tung, 1980. The concept of wave over-reflection and its application to baroclinic instability. J. Atmos. Sci., 37, 44-63.

Lindzen, R.S., B. Farrell and D. Jaqmin, 1981. Vacillations due to wave interference. Applications to the atmosphere and to annulus experiments. Submitted to J. Atmos. Sci.

Orr, W. McF., 1907. Stability or instability of the steady motions of a perfect liquid. Proc. Roy. Irish Acad. 27, 9-69.

Pedlosky, J., 1979. Geophysical Fluid Dynamics. Springer-Verlag, New York, 624 pp.

Pedlosky, J., 1970. Finite amplitude baroclinic waves. J. Atmos. Sci., 27, 15-30.

Pedlosky, J. 1964. An initial value problem in the theory of baroclinic instability. Tellus, 16, 12-17.

Sanders, F., and Gyakum, J., 1980. Synoptic-dynamic climatology of the "bomb." Mon. Wea. Rev., 108, 1589-1606.

Sawyer, J.S., 1961. Quasi-periodic variations with height in the lower stratosphere. Quart. J. Roy. Meteor. Soc. 87, 24-33.

Simmons, A.J. and Hoskins, B., 1978. The life cycles of some nonlinear baroclinic waves. J. Atmos. Sci., 25, 414-432.

Simmons, A.J., and Hoskins, B.J., 1979. The downstream and upstream development of unstable baroclinic waves. J. Atmos. Sci., 36, 1239-1254.

Stone, P.H., 1978. Baroclinic adjustment. J. Atmos. Sci., 35, 561-571.

Wilkinson, J.H., 1965. The algebraic eigenvalue problem. Clarendon Press, Oxford. 662 pp.